



The production and detection of Higgs particles at LEP

Guido Barbiellini, G. Bonneaud, G. Coignet, J. Ellis, M.K. Gaillard, J.-F. Grivaz, C. Matteuzzi, B.H. Wiik

► To cite this version:

Guido Barbiellini, G. Bonneaud, G. Coignet, J. Ellis, M.K. Gaillard, et al.. The production and detection of Higgs particles at LEP. 1979, 41 p. <in2p3-00775950>

HAL Id: in2p3-00775950

<http://hal.in2p3.fr/in2p3-00775950>

Submitted on 15 Jan 2013

HAL is a multi-disciplinary open access archive for the deposit and dissemination of scientific research documents, whether they are published or not. The documents may come from teaching and research institutions in France or abroad, or from public or private research centers.

L'archive ouverte pluridisciplinaire **HAL**, est destinée au dépôt et à la diffusion de documents scientifiques de niveau recherche, publiés ou non, émanant des établissements d'enseignement et de recherche français ou étrangers, des laboratoires publics ou privés.

DESY 79/27
May 1979



THE PRODUCTION AND DETECTION OF HIGGS PARTICLES AT LEP

ECFA/LEP Specialized Study Group 9 "Exotic Particles"

G. Barbiellini	-	INFN, Frascati and CERN
G. Bonneaud	-	Strasbourg and CERN
G. Coignet	-	LAPP, Annecy-le-vieux
J. Ellis	-	CERN
M. K. Gaillard	-	LAPP, Annecy-le-vieux
J. F. Grivaz	-	LAL, Orsay
C. Matteuzzi	-	CERN
B. H. Wiik	-	DESY

To be sure that your preprints are promptly included in the
HIGH ENERGY PHYSICS INDEX,
send them to the following address (if possible by air mail) :

DESY
Bibliothek
Notkestrasse 85
2 Hamburg 52
Germany

The Production and Detection of
Higgs Particles at LEP

ECFA/LEP Specialized Study Group 9
"Exotic Particles"

G.Barbiellini - INFN, Frascati and CERN
G.Bonneaud - Strasbourg and CERN
G.Coignet - LAPP, Annecy-le-vieux
J.Ellis - CERN
M.K.Gaillard - LAPP, Annecy-le-vieux
J.F.Grivaz - LAL, Orsay
C.Matteuzzi - CERN
B.H.Wiik - DESY

1. Introduction
 2. Neutral Higgs Particles
 - 2.1 Motivations and Properties
 - 2.2 $\text{Onium} \rightarrow \text{H}^0 + \gamma$
 - 2.3 $\text{Z}^0 \rightarrow \text{H}^0 + \gamma$
 - 2.4 $\text{Z}^0 \rightarrow \text{H}^0 + \mu^+ \mu^-$, $\text{H}^0 + e^+ e^-$
 - 2.5 $e^+ e^- \rightarrow \text{Z}^0 + \text{H}^0$
 - 2.6 Other reactions
 3. Charged Particles
 - 3.1 Motivations and Properties
 - 3.2 $e^+ e^- \rightarrow \text{H}^+ \text{H}^-$
 - 3.3 $e^+ e^- \rightarrow \text{W}^\pm \text{H}^\mp$
 - 3.4 Heavy Q $\rightarrow \text{H}^\pm + \text{Light } q$
 4. Conclusions
-

1. Introduction

Higgs particles are an inescapable ingredient of present gauge theories of the weak and electromagnetic interactions.¹ As such, their detection and study is of great importance and interest, both theoretical and experimental. Higgs particles are notoriously elusive², and it is certainly not obvious that any will have been found before LEP comes into operation. LEP will in any case provide unique opportunities to produce and detect Higgs particles and measure their couplings to quarks, leptons and intermediate vector bosons. These measurements would provide crucial tests of gauge theoretical ideas. In this report we review the different ways in which Higgs particles may be produced by LEP³, and discuss the principal experimental problems and backgrounds encountered in their detection. We make some judgements about the relative interest and utility of these different processes, which are in many cases strongly dependent on the (as yet unknown) masses of the Higgs particles. Section 2 deals with neutral Higgs bosons, principally the single particle H^0 encountered in the minimal version of the Weinberg-Salam model¹. First we review its couplings and decay modes² and phenomenological and theoretical restrictions on its mass. Then we discuss different processes for H^0 production with LEP, principally heavy $Q\bar{Q}$ onium $\rightarrow H^0 + \gamma$ ⁴, $Z^0 \rightarrow H^0 + \gamma$ ⁵ or $Z^0 \rightarrow H^0 + \ell^+\ell^-$ ⁶ and $e^+e^- \rightarrow Z^0 + H^0$ ⁷. In each case we present event rates and background calculations. Section 3 deals with charged Higgs bosons in a similar way. Their properties are less well-defined, and the corresponding phenomenological discussion less clear-cut. Among the reactions we consider are heavy quark or lepton decays to $H^\pm +$ light quark⁸, heavy quarkonium decays to $H^+ + H^- + X$, $e^+e^- \rightarrow H^+ + H^-$ and $e^+e^- \rightarrow H^\pm + W^\mp$ ⁹. Section 4 summarizes our tentative conclusions about the prospects for different modes of Higgs production and detection with LEP.

2. Neutral Higgs Particles

2.1. Motivations and Properties

The present interest in gauge theories of the weak and electromagnetic interactions stems largely from their ability to make precise predictions which have a knack of agreeing with experiment. This precision is a consequence of the calculability of higher order effects which results from the renormalizability of gauge theories¹⁰. The old four-fermion model of the weak interactions had many infinities in higher orders which forbade its serious consideration as a fundamental theory. A lot of these infinities were alleviated by the introduction of intermediate vector bosons, and the situation was further improved by making them into a gauge theory with its characteristic 3- and 4-boson couplings. There were still residual infinities which were finally removed by introducing Higgs fields and generating vector boson masses by spontaneous symmetry breaking¹. Indeed, it has been shown that this is essentially the only way of obtaining a calculable theory of the weak interactions which is renormalizable in perturbation theory¹¹. All weak interaction theories have at least one physical Higgs particle, and we see that its detection is a crucial test of the entire gauge philosophy. Although many people¹² would like to replace fundamental Higgs fields by some form of dynamical symmetry breaking, no fully realistic model yet exists. It might well be that such a scheme would contain bound states with properties analogous to those of conventional Higgs particles: no theories exist to prove or disprove such a possibility.

Let us discuss the single neutral Higgs boson present in the minimal Weinberg-Salam model^{1,2,7}. This model starts with a single complex Higgs multiplet, which transforms as a doublet under weak SU(2):

$$\phi = \begin{pmatrix} \phi^+ \\ \phi^0 \end{pmatrix} \quad (2.1)$$

which plays with itself via a Higgs potential as in fig. 1a

$$(V\phi) = -\mu^2 |\phi|^2 + \lambda |\phi|^4 \quad (2.2)$$

The minimum of this potential is situated at

$$|\phi|^2 = \mu^2/2\lambda \equiv v^2/2 \quad (2.3)$$

and normal perturbation theory is an expansion in

$$\phi' = \phi - \phi_{\min} \quad (2.4)$$

where ϕ_{\min} minimizes the potential (2.2) and can be taken in the form

$$\phi_{\min} = \begin{pmatrix} 0 \\ \frac{v}{\sqrt{2}} \end{pmatrix} \quad (2.5)$$

Of the four real fields represented by (2.1) and its complex conjugate ϕ^+ , $\phi^- \equiv \phi^+$ and $\chi \equiv (\phi^0 - \bar{\phi}^0)/\sqrt{2}$ disappear from the theory as physical particles, becoming longitudinal polarization components of the massive vector bosons. There is just one physical Higgs particle which can be written² as

$$H^0 = \frac{\phi^0 + \bar{\phi}^0}{\sqrt{2}} - v \quad (2.6)$$

The coupling of H^0 to other particles are simply given by their masses. Consider the Higgs-fermion coupling

$$\frac{g_{fH}}{\sqrt{2}} \bar{f}f\phi^0 + (\text{hermitian conjugate}) \rightarrow g_{fH} \bar{f}f(H^0 + v) = g_{fH} \bar{f}fH^0 + m_f \bar{f}f \quad (2.7)$$

Equation (2.7) immediately entails that

$$g_{fH} = \frac{m_f}{v} \quad (2.8)$$

proportional to the fermion (quark or lepton) mass. Correspondingly, the $H^0 W^+ W^-$ coupling

$$\begin{aligned} \frac{g^2}{2} W_\mu^+ W_\mu^- |\phi|^2 &\rightarrow \frac{g^2}{4} W_\mu^+ W_\mu^- (H^{02} + 2vH^0 + v^2) \\ &= \frac{g^2}{4} H^{02} W_\mu^+ W_\mu^- + g_{WH} H^0 W_\mu^+ W_\mu^- + m_W^2 W_\mu^+ W_\mu^- \end{aligned} \quad (2.9)$$

from which it follows that

$$g_{WH} = \frac{2m_W^2}{v} \quad (2.10)$$

and

$$v^2 = \frac{4m_W^2}{g} \quad (2.11)$$

Remembering also that in the Weinberg-Salam model¹

$$\frac{G_F}{\sqrt{2}} = \frac{g^2}{8m_W^2} + v^2 = \frac{1}{\sqrt{2}G_F} \quad (2.12)$$

we see that the couplings of the Weinberg-Salam Higgs boson are completely determined

$$\text{for fermions: } g_{fH} = 2^{1/4} \sqrt{G_F} m_f \approx 3.8 \times 10^{-3} \left(\frac{m_f}{m_{\text{proton}}} \right) \quad (2.13)$$

$$\text{for vector bosons: } g_{vH} = 2^{5/4} \sqrt{G_F} m_v^2 \approx 7.6 \times 10^{-3} \left(\frac{m_v^2}{m_{\text{proton}}^2} \right)$$

By contrast, the mass of the Higgs boson is almost completely undetermined. The potential (2.2) implies that

$$m_H^2 = 2\mu^2 = 2\lambda v^2 \quad (2.14)$$

There is an experimental constraint on v (2.12), but the individual values of μ and λ are relatively unconstrained. In order for perturbation theory to be applicable, λ should not be too large, and the relation (2.14) therefore suggests an upper bound on m_H , which is found¹³ to be

$$M_H \lesssim 1 \text{ TeV} \quad (2.15)$$

How about a lower limit on m_H ? Various phenomenological nuclear physics constraints entail⁷

$$M_H \gtrsim 15 \text{ MeV} \quad (2.16)$$

In fact the formula (2.14) is not applicable when M_H (or μ , or λ) is arbitrarily small, because radiative corrections to the Higgs potential λ become important. For very small μ^2 as in fig. 1b (and there are aesthetic preferences for $\mu^2 = 0$ ^{15,16})

$$m_H^2 \approx \frac{3g^2}{8} v^2 \left\{ \frac{2 + \sec^4 \theta_W}{\sin^4 \theta_W} - 0 \left(\frac{m_f}{m_W} \right)^4 \right\} \quad (2.17)$$

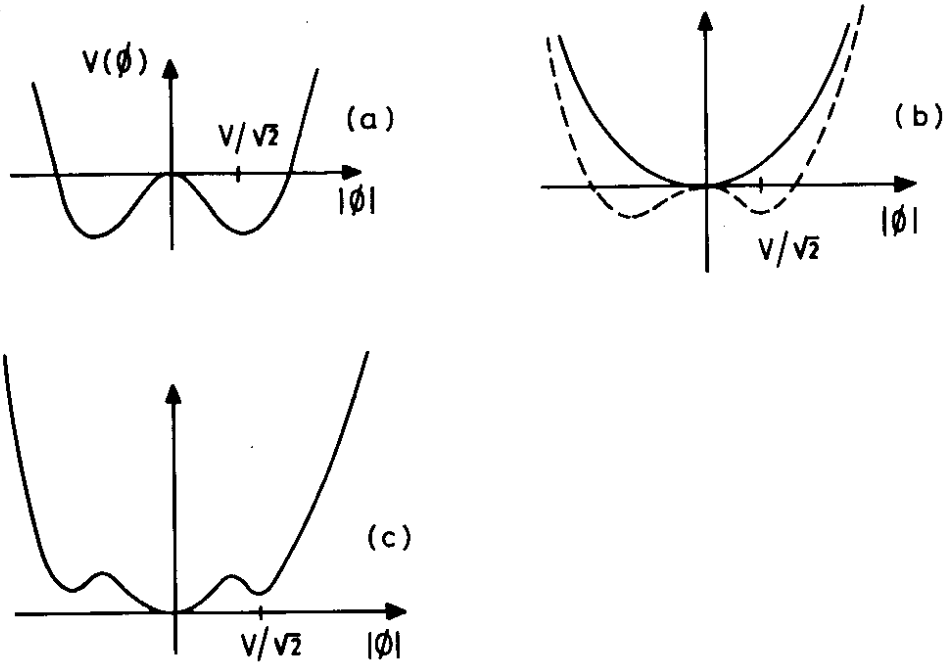


Fig. 1 - The shape of the Higgs potential for different values of μ^2 : (a) $\mu^2 > 0$; (b) $\mu^2 = 0$ with the effect of radiative corrections indicated by the dashed line; (c) $\mu^2 < 0$ with the local minimum at $|\phi| = v/\sqrt{2}$ not an absolute minimum

corresponding to

$$m_H = 10.4^{+0.5}_{-0.4} \text{ GeV for } \sin^2\theta_W = 0.20 \pm 0.01 \quad (2.18)$$

if the fermion mass contributions in (2.17) are negligible ($\Delta m_H \leq 6 \text{ MeV}$ for $m_t \lesssim 15 \text{ MeV}$). In fact the absolute minimum of the radiatively corrected Higgs potential could still be controlled by the radiative corrections and situated at $\phi_{\min} \neq 0$ even if μ^2 is slightly negative. The requirement that the absolute minimum be at $\phi_{\min} \neq 0$ gives an upper bound on $(-\mu^2)$ which in turn gives a lower bound

$$m_H \gtrsim 7.35 \text{ GeV for } \sin^2\theta_W = 0.20 \quad (2.19)$$

Conceivably¹⁸, the theory could be sitting at a local minimum of $v(\phi)$ which was not an absolute minimum, as in fig. 1c. The universe would then be unstable, but the decay from local to absolute minimum would be sufficiently slow (lifetime greater than the lifetime of the universe $\sim 10^{10}$ years) if¹⁹

$$m_H \gtrsim 260 \text{ MeV} \quad (2.20)$$

Clearly, finding a Higgs with a mass between (2.19) and (2.20) would have cosmic implications: finding one below (2.20) would be distinctly worrying! A baseless theoretical guess of the relative probability of finding the Higgs in any given logarithmic mass range is indicated in fig. 2.

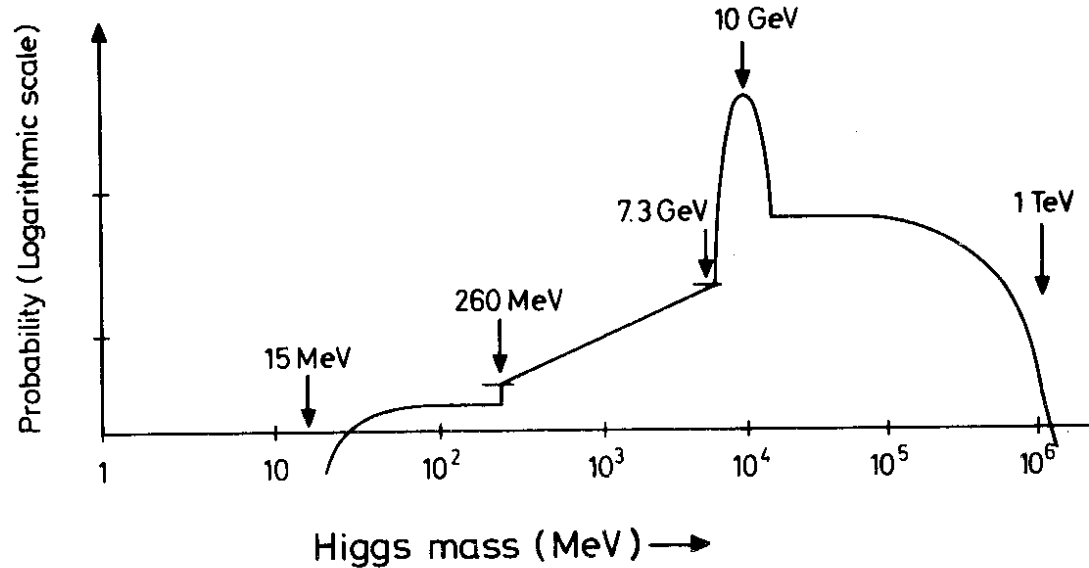


Fig. 2 - A guess at the probability of finding a Higgs boson with a given mass on a logarithmic scale

The precise predictions (2.13) of the Higgs couplings enable its decay modes to be reliably estimated ⁷ as a function of its mass, as shown in fig. 3, which should be supplemented by the following remarks. For m_H in the neighbourhood of 10 GeV as suggested by (2.18), the decay modes are somewhat more complicated ¹⁶ as indicated in fig. 4. The decays $H^0 \rightarrow \tau^+\tau^-$ and $c\bar{c}$ dominate for $4 \text{ GeV} < m_H < 12 \text{ GeV}$, while $H^0 \rightarrow b\bar{b}$ dominates for $m_H > 12 \text{ GeV}$, and $H^0 \rightarrow t\bar{t}$ for m_H above the $t\bar{t}$ threshold. The decays $H^0 \rightarrow W^+W^-$ and Z^0Z^0 dominate for $m_H > 200 \text{ GeV}$, unless there is some very heavy fermion with $m_f \gtrsim m_{W,Z}$. These considerations at least tell us what signatures to look for, even if we do not know what mass range the Higgs boson may occupy.

Good signatures seem to be

$4 \text{ GeV} < m_H < 12 \text{ GeV}$: $H^0 \rightarrow \tau^+\tau^-$, decays to $\mu^+\mu^-$ are much suppressed with a branching ratio $O(10^{-3})$.

$12 \text{ GeV} < m_H < 200 \text{ GeV}$: Decays into the heaviest QQ^- (or heavy L^+L^-) pair kinematically acceptable. This is a unique signature which suggests that H^0 decays may contain many prompt leptons and/or strange particles and have relatively high sphericity (low thrust).

We now turn to our discussions of H^0 production mechanisms.

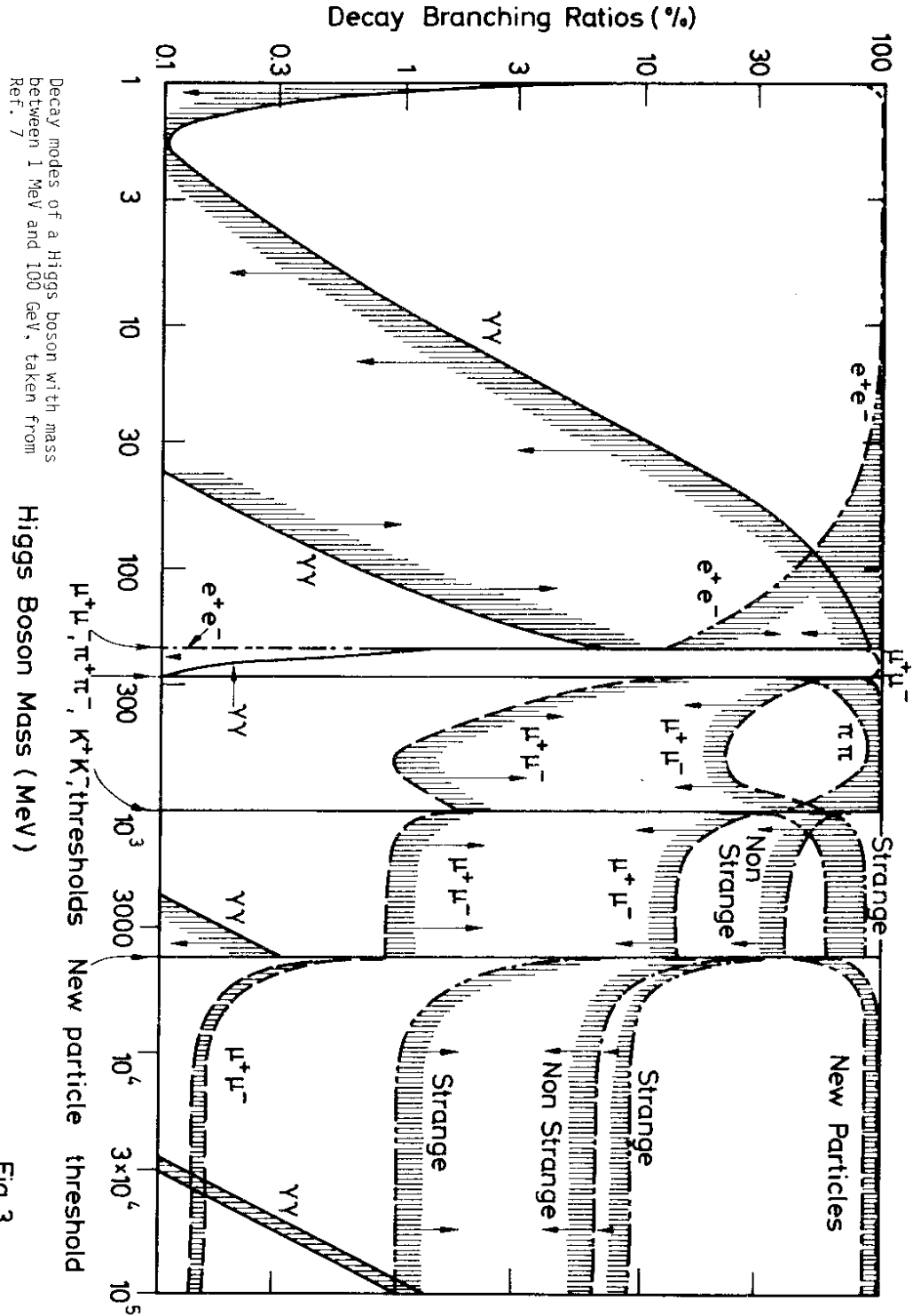


Fig. 3

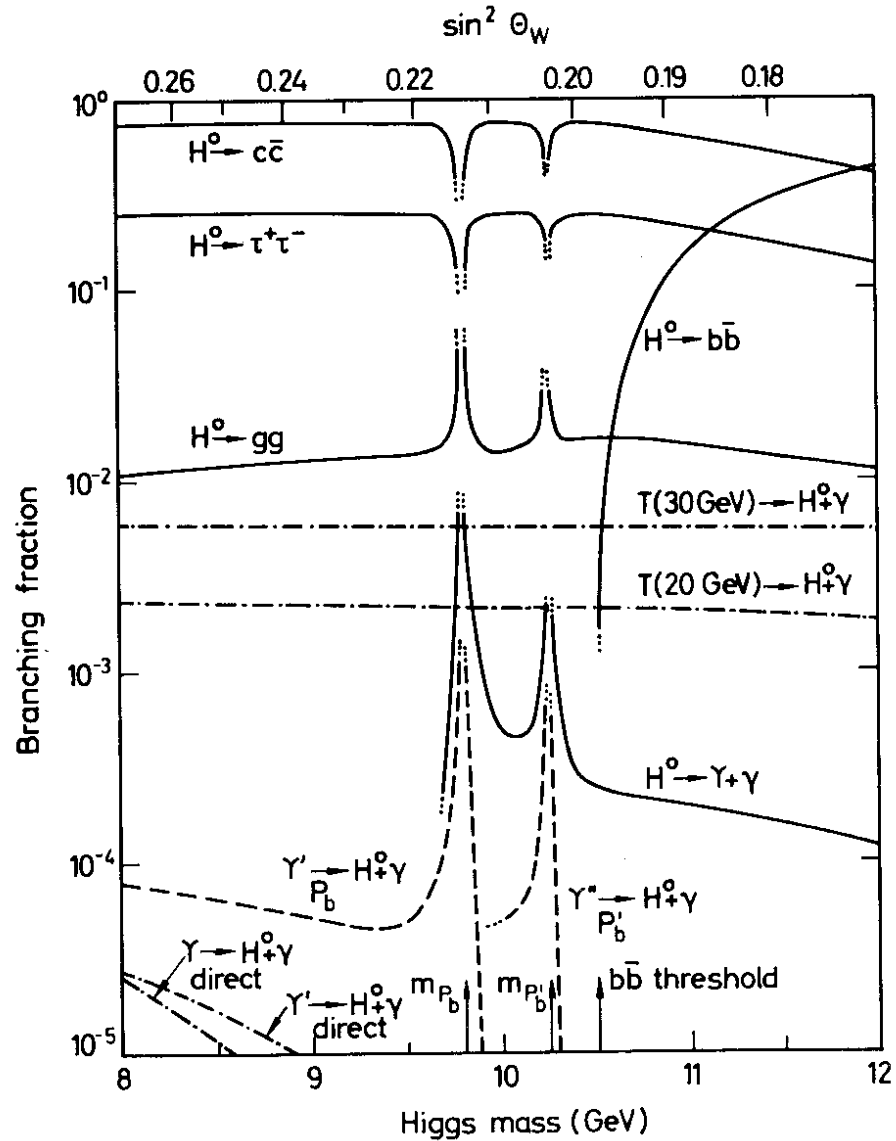


Fig. 4

Decay modes and production rates of a Higgs boson with mass around 10 GeV, taken from Ref. 16

2.2 Onium $\rightarrow H^0 + \gamma$

The decay of a heavy $Q\bar{Q}$ (1^{--}) state into $H^0 + \gamma$ should be observably large⁴. The Higgs can couple directly to the heavy constituent quark and rival decay modes are suppressed by the Zweig rule (see fig. 5). The decay rate is¹⁶

$$\frac{\Gamma(V \rightarrow H^0 + \gamma)}{\Gamma(V \rightarrow \gamma + \ell^+ \ell^-)} \approx \frac{G_F m_V^2}{4\sqrt{2} \pi \alpha} \left[1 - \frac{m_H^2}{m_V^2} \right] \quad (2.21)$$

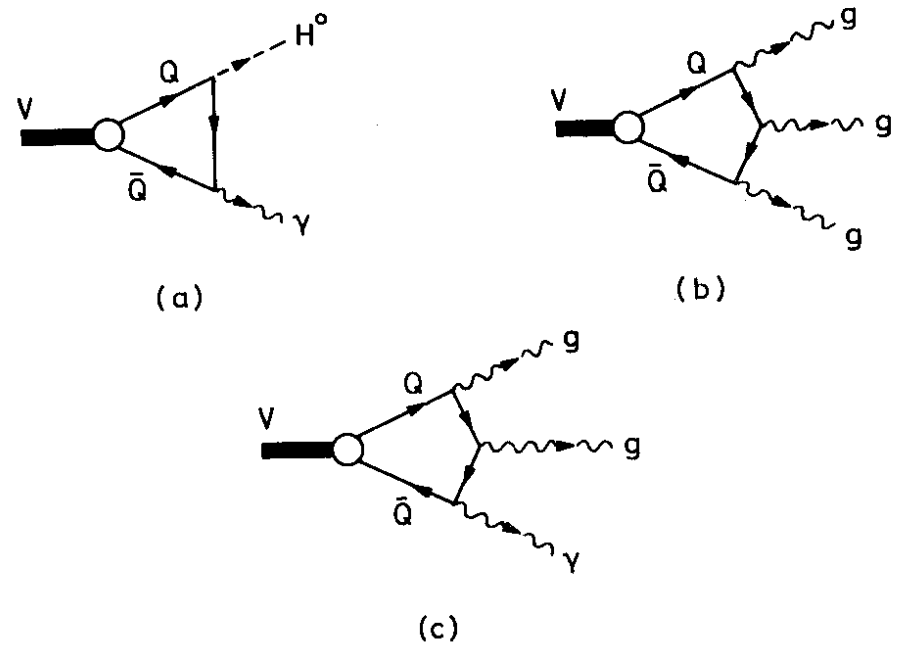


Fig. 5 - Onium decays into (a) $H^0 + \gamma$, (b) the dominant Zweig-suppressed hadronic decay into 3 gluons, and (c) $\gamma + 2$ gluons

For m_H sufficiently lighter than m_V that the $Q\bar{Q}$ binding energy can be neglected: $|2m_Q - m_V| \ll |m_H - m_V|$. The ratio (2.21) is already 8% for $m_V \approx 30$ GeV, and becomes $O(1)$ for any onium in the LEP energy range. The rate for $e^+e^- \rightarrow V \rightarrow H^0 + \gamma$ depends very sensitively on m_V and on uncertainties in rival decay modes of the onium. If we take as an example $m_V \approx 100$ GeV, corresponding to $O(100)$ onium events/day²⁰, then $\Gamma(V \rightarrow H^0 + \gamma) / \Gamma(V \rightarrow \gamma + e^+e^-) \approx 0.9$ giving a Higgs production rate of (1 to 10)/day.

The principal background to $V \rightarrow H^0 + \gamma$ is expected to come from the process $V \rightarrow \gamma + 2$ gluons (fig. 5c) for which the decay rate is

$$\frac{\Gamma(V \rightarrow \gamma + 2 \text{ gluons})}{\Gamma(V \rightarrow \gamma + e^+e^-)} \approx \frac{8(\pi^2 - 9)}{9\pi} \frac{\alpha_s^2}{\alpha} \quad (2.22)$$

which is 1 for $\alpha_s \approx 0.17$, a reasonable median value for foreseeable onia.

The γ spectrum in $V \rightarrow \gamma + 2$ gluons is approximately linear, so we take it to be

$$\frac{1}{\Gamma(V \rightarrow \gamma + e^+e^-)} \frac{d\Gamma(V \rightarrow H + \gamma)}{dX_Y} \approx 2X_Y \quad (2.23)$$

Taking the photon energy resolution to be

$$\frac{\Delta E_Y}{E_Y} = \frac{\Delta X_Y}{X_Y} = \frac{0.1}{\sqrt{E_Y}} \quad (2.24)$$

we find that the background under a Higgs signal is approximately

$$\frac{1}{\Gamma_{e^+e^-}} \frac{d\Gamma}{dX_Y} \Delta X_Y = \frac{0.28 X_Y^{3/2}}{\sqrt{m_V}} : X_Y = \left(1 - \frac{m_H^2}{m_V^2}\right) \quad (2.25)$$

Comparing the expression (2.25) and (2.21) we see that the signal to background ratio will be >1 already for an onium at the top end of the PEP-PETRA range $m_V = 30$ GeV, and that the situation is much better for any onia in the LEP range. Furthermore, one can use decay signatures to enhance the $H^0 + \gamma$ signal, such as looking for $H^0 \rightarrow \tau^+\tau^-$ or $H^0 \rightarrow c\bar{c}, b\bar{b}$ which are probably negligible decay modes of the digluon system in $V \rightarrow \gamma + 2$ gluons. In particular, $H \rightarrow \tau^+\tau^-$ would be a distinctive signature, with a branching ratio $\geq 25\%$ for $m_H < 12$ GeV, and $\geq 2\%$ for $12 \text{ GeV} < m_H < 2m_t$. We therefore feel that if there is an onium system in the LEP energy range it will be easy to use it to scan for a H^0 with $m_H < m_V$. By the same token an onium in the PEP-PETRA energy range would also enable a search of the low-mass range of m_H .

The only complication might arise if the H^0 had a mass close to that of some other onium system, e.g. a 10 GeV Higgs would lie in the middle of the bottomonium¹⁶ spectrum. In this case one would need to devise tests to ensure one was observing $V \rightarrow H + \gamma$, and not $V \rightarrow \gamma +$ some P-wave bottomonium state. This could be done by pinpointing the $H \rightarrow \tau^+\tau^-$ decay mode, which would be negligible for P-wave onia.

Onium decays are very suitable for looking for sufficiently light Higgs mesons.

2.3 $Z^0 \rightarrow H^0 + \gamma$

LEP will have a very high event rate ²⁰ at the Z^0 resonance, enabling event samples of $O(10^6 \text{ to } 10^7)$ Z^0 decays. It is therefore natural to consider rare Z^0 decays as a source of Higgs boson production. The process $e^+e^- \rightarrow H^0 + \gamma$ ⁵ has a clean signature in the outgoing monochromatic photon, as in the previous $V \rightarrow H + \gamma$ decay. Unfortunately, in this case $Z^0 \rightarrow H^0 + \gamma$ vanishes in lowest order and the process only occurs through higher order diagrams where fermion and W^\pm boson loops contribute (see fig. 6). So although the coupling of the Higgs boson to the vector bosons is very large (2.13) being proportional to the vector boson mass squared, the rate for this process remains very low. The rate ⁵ (see fig. 7):

$$\frac{\Gamma(Z^0 \rightarrow H^0 + \gamma)}{\Gamma(Z^0 \rightarrow \mu^+ \mu^-)} \approx 7.8 \times 10^{-5} \left(1 - \frac{m_H^2}{m_Z^2}\right)^3 \left(1 + 0.17 \frac{m_H^2}{m_Z^2}\right) \quad (2.26)$$

has been calculated from the W^\pm boson loop alone, yielding a branching ratio $B(Z^0 \rightarrow H^0 + \gamma) \approx 10^{-6}$ for $m_H \ll m_Z$. This calculation is a non-trivial check on the gauge structure of the theory, and may be modified if the gauge group is bigger than $SU(2) \times U(1)$. If some quark and/or lepton flavours at least as heavy as the W^\pm exist, the fermion loop contribution also becomes important and the rate of $Z^0 \rightarrow H^0 + \gamma$ counts the number of heavy quark flavours. Unfortunately, for $\sin^2 \theta_W < 3/8$ in the Weinberg-Salam model the interference between fermion and W^\pm loops is destructive and the decay rate is decreased unless N_a , the number of generations of heavy fermions, is large:

$$\Gamma(Z^0 \rightarrow H^0 + \gamma) \sim |1 - N_a/7|^2 \quad \text{for } \sin^2 \theta_W = 0.20 \quad (2.27)$$

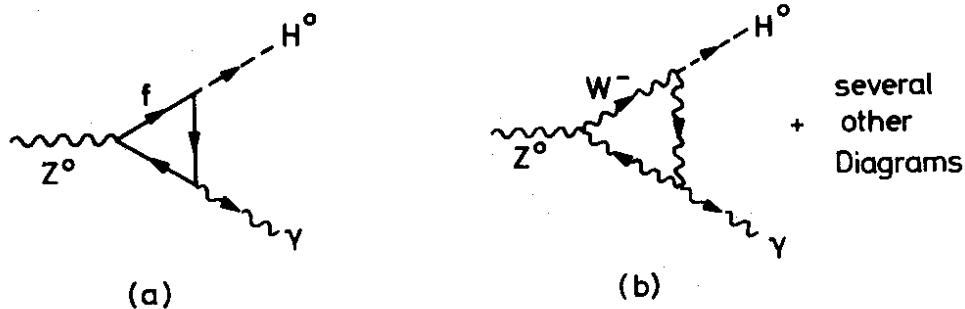
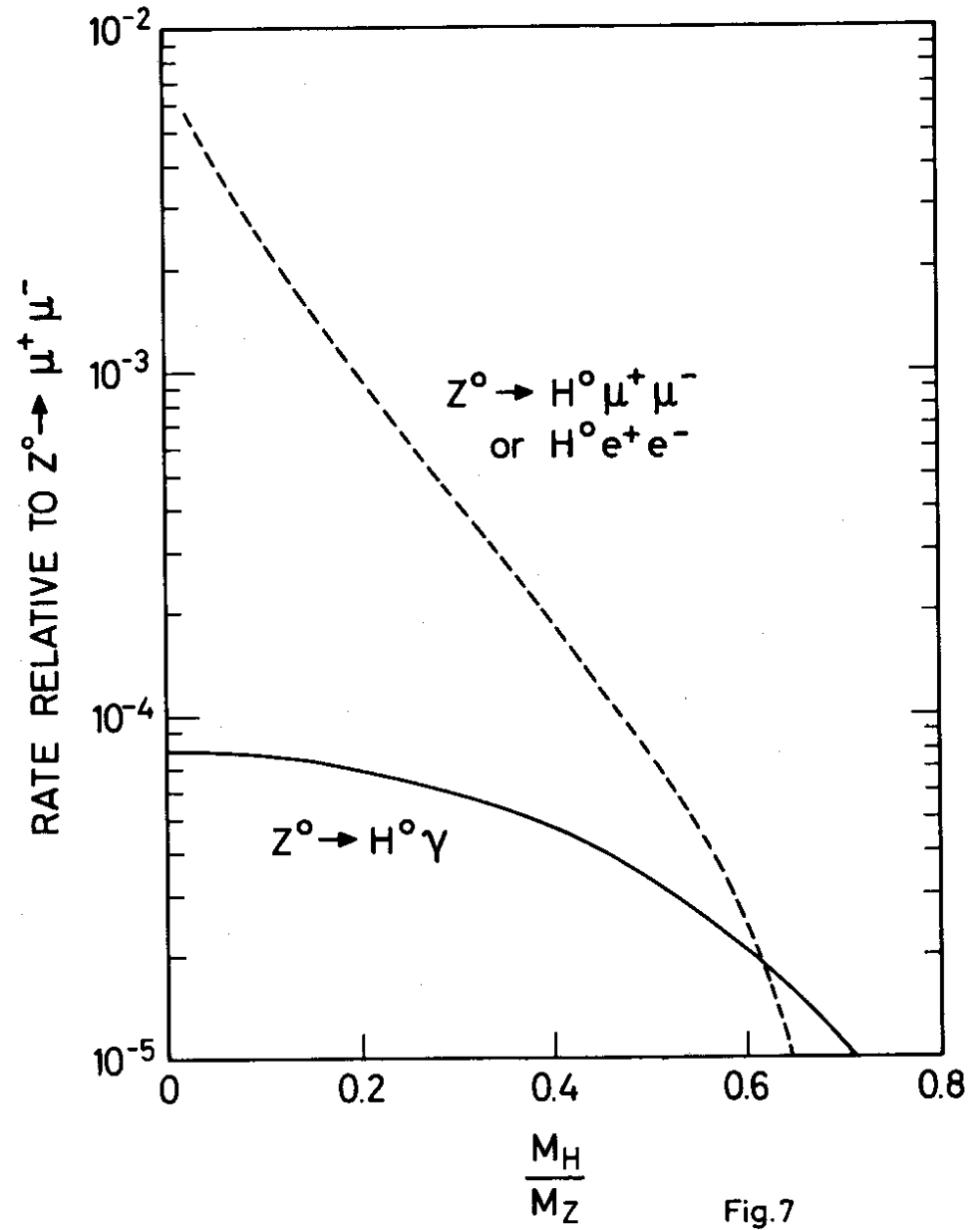


Fig. 6 - Contribution to $Z^0 \rightarrow H^0 + \gamma$ decay from (a) a fermion loop. (b) a W^\pm loop.



Decay rates for $\Gamma(Z^0 \rightarrow H^0 + \gamma)/\Gamma(Z^0 \rightarrow \mu^+ \mu^-)$ and $\Gamma(Z^0 \rightarrow H^0 + \mu^+ \mu^- \text{ or } e^+ e^-)/\Gamma(Z^0 \rightarrow \mu^+ \mu^-)$ for different values of m_H/m_Z taken from Ref. 5.

To assess the background to a hunt for $Z^0 \rightarrow H^0 + \gamma$ we consider the two reactions $e^+e^- \rightarrow L^+L^-\gamma$ (where L is a heavy lepton) and $e^+e^- \rightarrow Q\bar{Q}\gamma$ (where Q is a heavy quark), since the dominant H^0 decays are likely to be to L^+L^- or $Q\bar{Q}$. In the case of $e^+e^- \rightarrow L^+L^-$ we only need to consider pure QED diagrams. In estimating the background we have neglected radiation from the incoming e^+e^- lines, which would be sharply peaked along the beam directions and probably negligible at the Z^0 peak. We have further used

$$\frac{d\Gamma(Z^0 \rightarrow L^+L^-\gamma)}{\Gamma(Z^0 \rightarrow \mu^+\mu^-)} \approx \frac{d\Gamma(Z^0 \rightarrow L^+L^-\gamma)}{\Gamma(Z^0 \rightarrow L^+L^-)} \frac{\text{Phase space } (Z^0 \rightarrow L^+L^-)}{\text{Phase space } (Z^0 \rightarrow \mu^+\mu^-)} \quad (2.27)$$

and standard QED formulae for $e^+e^- \rightarrow L^+L^-\gamma$ to estimate $d\Gamma(Z^0 \rightarrow L^+L^-\gamma)$. The curves μ , τ and L ($m_L = 10$ GeV) in Fig. 8 represent $d\Gamma$ multiplied by the energy resolution for a photon, again assumed to be (2.24) $\Delta E_\gamma/E_\gamma \approx 0.1/E_\gamma$. These curves clearly lie far above the signal for $Z^0 \rightarrow H^0 + \gamma$, even before taking account of the $H^0 \rightarrow L^+L^-$ branching ratio. However, the photons emitted in $e^+e^- \rightarrow L^+L^-\gamma$ will tend to be emitted parallel to the outgoing L^\pm lines. To attempt to reduce the background we have shown the effect of selecting events where both L^\pm go into the same hemisphere opposite the γ . The full curves μ , τ and L now become the dashed lines. The $H^0 + \gamma$ signal is also reduced by such a cut, to the curves A (for $H^0 \rightarrow \mu^+\mu^-$, $\tau^+\tau^-$) or B (for $H^0 \rightarrow L^+L^-$: $m_L = 10$ GeV).

While the background is substantially reduced, and the signal not badly reduced for $m_H/m_Z < 1/2$, the signal to background ratio is still very low. The situation might be acceptable for a 10 GeV Higgs $\rightarrow \tau^+\tau^-$, but such a Higgs could be more easily seen elsewhere. Looking for a heavier Higgs by $Z^0 \rightarrow H^0 + \gamma$ looks very difficult. Similar remarks apply to trying to detect $Z^0 \rightarrow H^0 + \gamma$ against a background of radiative decays $Z^0 \rightarrow Q\bar{Q} + \gamma$.

We conclude that $Z^0 \rightarrow H^0 + \gamma$ is not a good way to search for the Higgs boson. However, the reaction is of considerable importance as a probe of gauge theory structure, and would be an interesting reaction to study if the Higgs boson had been identified in some other reaction.

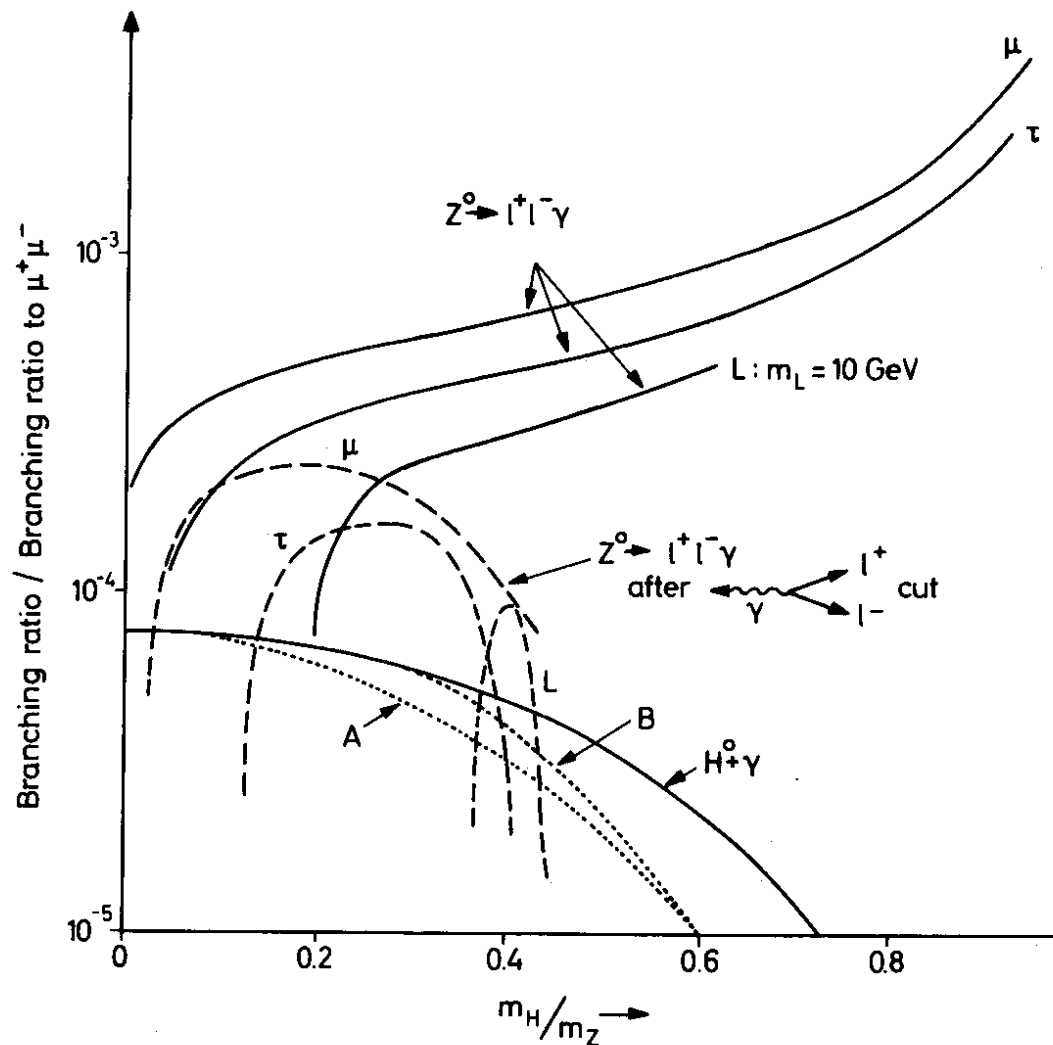


Fig. 8

The $Z^0 \rightarrow l^+l^-$ background to the search for $Z^0 \rightarrow H^0 + \gamma$. The labelling of the curves is explained in the text

2.4 $Z^0 \rightarrow H^0 + \mu^+\mu^-, H^0 + e^+e^-$

The dominant contribution to these decays is expected to come from $Z^0 \rightarrow H^0 + Z^0_{\text{virtual}}$, with $Z^0_{\text{virtual}} \rightarrow \mu^+\mu^-$ or e^+e^- (as in Fig. 9). In principle one could also look for $Z^0_{\text{virtual}} \rightarrow q\bar{q}$, but it is not clear how separate this process from the bulk of hadronic Z^0 decays. The total rate for $Z^0 \rightarrow H^0 + \ell^+\ell^-$ from this reaction is ⁶ given by

$$\frac{1}{\Gamma(Z^0 \rightarrow \mu^+\mu^-)} \frac{d\Gamma(Z^0 \rightarrow H^0 + \ell^+\ell^-)}{dx_H} = \frac{\alpha}{4\pi \sin^2\theta_W \cdot \cos^2\theta_W} \frac{\left[1 - X_H + \frac{X_H^2}{12} + \frac{2}{3} \frac{m_H^2}{m_Z^2}\right] \left[X_H^2 - \frac{4m_H^2}{m_Z^2}\right]^{1/2}}{\left[X_H - \frac{m_H}{m_Z}\right]^2} \quad (2.28)$$

where $X_H \equiv 2E_H/m_Z$. The rate given by (2.28) as a function of m_H is plotted in Fig. 7. Recalling that $B(Z^0 \rightarrow \mu^+\mu^-) \approx 3\%$, we see that at $m_H \sim m_Z/2 \sim 50$ GeV the branching ratio $B(Z^0 \rightarrow H^0 + \ell^+\ell^-) \sim 10^{-6}$, corresponding²⁰ to about 1 event per week, which maybe is the limit of experimental detectability. An interesting feature of this decay is that the $(\ell^+\ell^-)$ invariant mass spectrum is peaked towards high invariant masses²¹. This is shown in Fig. 10, where we see that the peak in the $\kappa \equiv (m_{\ell^+\ell^-}/m_Z)$ spectrum occurs at $\kappa = 0.95 (m_H/m_Z)$. (2.29)

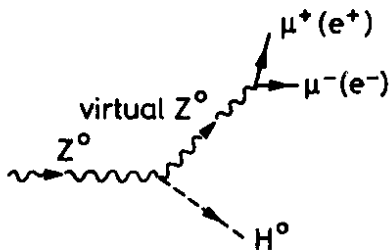
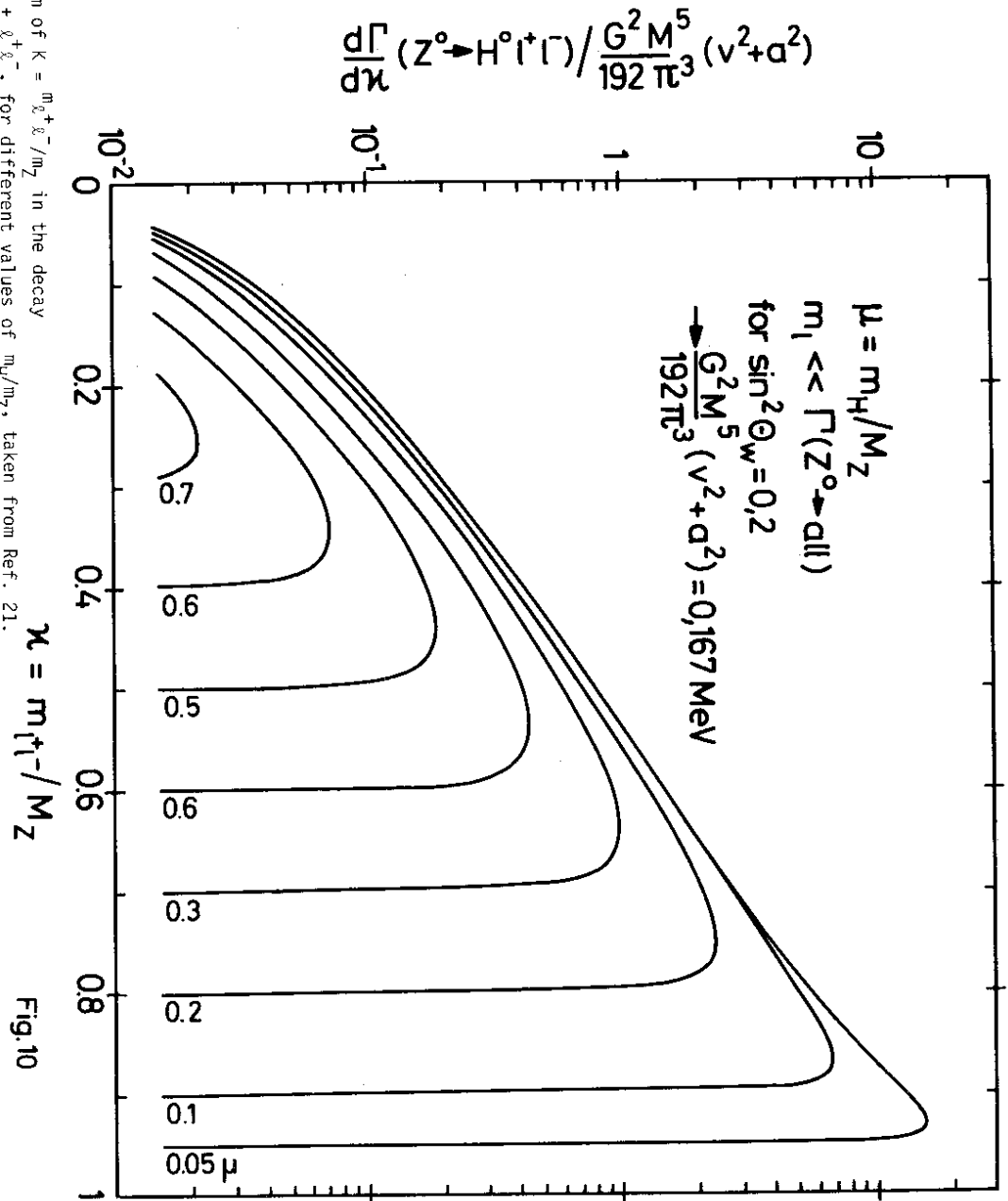


Fig. 9 - Dominant Diagram for $Z^0 \rightarrow H^0 + \mu^+\mu^-$ or e^+e^-

Spectrum of $\kappa = m_{\ell^+\ell^-}/m_Z$ in the decay $Z^0 \rightarrow H^0 + \ell^+\ell^-$, for different values of m_H/m_Z , taken from Ref. 21.



The resolution in m_H is likely to be better if one observes $Z^0 \rightarrow H^0 + (e^+e^-)$ rather than $H^0 + (\mu^+\mu^-)$. In general one has

$$\frac{\Delta X}{X} \approx \frac{1}{2} \left(\frac{\Delta E_{1+}}{E_{1+}} + \frac{\Delta E_{1-}}{E_{1-}} \right) \approx \frac{\Delta E_1}{E_1} \quad (2.30)$$

since $E_{\ell^+} \approx E_{\ell^-}$. For e^\pm we expect

$$\frac{\Delta E_e}{E_e} \approx \frac{0.1}{\sqrt{E_e}} \quad (2.31)$$

whereas for μ^\pm we expect

$$\frac{\Delta E_\mu}{E_\mu} \approx 0.15 \gg \frac{\Delta E_e}{E_e} \quad (2.32)$$

The error on m_H is directly related to $\Delta\kappa$

by
$$\Delta m_H \approx \frac{\kappa(\Delta\kappa)}{m_H} \quad (2.33)$$

from which we eventually get for $Z^0 \rightarrow H^0 + (e^+e^-)$:

$$\Delta m_H \approx 0.14 m_H^{1/2} \left(0.95 \frac{m_Z}{m_H} - 1 \right)^{3/2} \quad (2.234)$$

The numerical values of this formula are tabulated below:

(all masses in GeV)

m_H	10	20	30	40	50
Δm_H	10	4	2	~ 1	~ 1

We see that the mass resolution is interestingly small for $m_H > 20$ GeV. Other production mechanisms are likely to give better resolution for $m_H < 20$ GeV (e.g. the $V \rightarrow H^0 + \gamma$ of section 2.2, the reaction $e^+e^- \rightarrow Z^0 + H^0$ of section 2.5). The backgrounds to this reaction seem likely to be negligible, at least for $m_H > 30$ GeV.

Electromagnetic production of hadrons + $(\ell^+\ell^-)$ pairs will be peaked towards low invariant masses, rather than the high masses (fig. 10) associated with $Z^0 \rightarrow H + \ell^+\ell^-$. Also, many of the electromagnetic $\ell^+\ell^-$ pairs will be emitted in the outgoing $q\bar{q}$ jet directions, whereas the ℓ^+ from $Z^0 \rightarrow H^0 + \ell^+\ell^-$ will be coming out at large angles relative to the decay products of the Higgs. By comparison with the $Z^0 \rightarrow H^0 + \gamma$ process discussed previously in section (2.3), fig. 7 shows that the signal is larger for $m_H < 50$ GeV whereas the electromagnetic background is suppressed by an extra power of $(\frac{\alpha}{\pi})$, as well as the kinematic effects mentioned above. More serious than the electromagnetic background might be that from weak decays :

$$Z^0 \rightarrow Q + \bar{Q} \rightarrow \mu^+\mu^- \nu\bar{\nu} X$$

However, these reactions will in general have substantial missing energy and momentum because of the missing neutrinos. It should therefore be relatively easy to remove these events by a calorimetric cut on the total energy

$$E_{\text{hadrons}} + E_{\ell^+} + E_{\ell^-} = m_Z \quad (2.35)$$

We have not studied this problem in detail because it would seem to take us too far into the design of a LEP detector. Nevertheless, it seems to us that the rate and signature for $Z^0 \rightarrow H^0 + e^+e^-$ is sufficiently good for a Higgs to be found if $20 \text{ GeV} < m_H < 50 \text{ GeV}$. For a lower mass Higgs the reaction is less attractive because of problems with the mass resolution, if this is indeed determined by the e^\pm measurement errors. Note however that in the case of a low-mass Higgs the e^+e^- invariant mass (2.29) is relatively large, so that the backgrounds are likely to be small, and the signal is of course larger for lighter m_H .

2.5 $e^+e^- \rightarrow Z^0 + H^0$

In this reaction the basic mechanism is the bremsstrahlung process $e^+e^- \rightarrow Z^0_{\text{virtual}} \rightarrow Z^0 + H^0$ indicated in Fig. 11⁷.

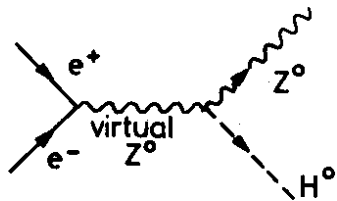


Fig. 11 - Dominant Diagram for $e^+e^- \rightarrow Z^0 + H^0$

For Higgs which are relatively light compared with the Z^0 ,

$$\frac{\sigma(Z^0 + H^0)}{\sigma_{\text{pt}}} \quad (\text{where } \sigma_{\text{pt}} \equiv \frac{4\pi\alpha^2}{3s} = \frac{87 \text{ nb}}{s} \text{ is the point-like QED cross-section})$$

reaches a peak at $\sqrt{s} = m_Z + \sqrt{2} m_H$:

$$\frac{\sigma(Z^0 + H^0)}{\sigma_{\text{pt}}} = \frac{3}{64} \left(\frac{m_Z}{38 \text{ GeV}} \right)^4 \frac{m_Z}{2\sqrt{2}m_H} \left(1 + \frac{v^2}{a^2} \right) \quad (2.36)$$

where for $\sin^2\theta_W \approx 0.20$, $m_Z \approx 90 \text{ GeV}$ and $v/a = -0.2$ so that

$$\frac{\sigma(Z^0 + H^0)}{\sigma_{\text{pt}}} = \frac{47}{m_H(\text{GeV})} \quad (2.27)$$

at peak²². In order to have a good signature of the mass m_H defined by

$$m_H^2 = (\sqrt{s} - E_Z)^2 - p_Z^2 \quad (2.38)$$

only the cleanest decays of the Z^0 , namely $Z^0 \rightarrow e^+e^-$ and perhaps $Z^0 \rightarrow \mu^+\mu^-$, will be considered. With the branching ratio $B(Z^0 \rightarrow e^+e^-) \sim 3\%$ folded in, we find the event rates per day listed below, for Higgs masses between 10 and 60 GeV assuming a luminosity of $10^{32} \text{ cm}^{-2} \text{ sec}^{-1}$.

Table: Rates for $e^+e^- \rightarrow Z^0 + H^0$

$m_H(\text{GeV})$	$\sqrt{s}(\text{GeV})$	$\frac{\sigma(Z^0 + H^0)}{\sigma_{\text{pt}}}$	$\# (H^0 + Z^0)$ per day	$\# (H^0 + e^+e^-)$ per day
10	104	4.70	350	10.5
30	132	1.56	67	2
45	154	1.04	32	1
60	175	0.78	19	0.6

We therefore find a useful event rate (1)/day which varies by about an order of magnitude over the mass range considered. The ratios $\sigma(Z^0 + H^0)/\sigma_{\text{pt}}$ for other values of s and m_H are plotted²² in Fig. 12

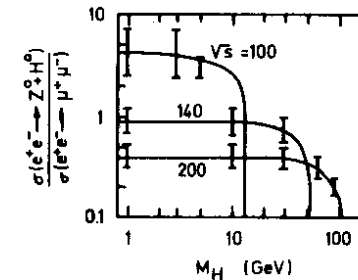


Fig. 12 - Cross-section ratios $\sigma(e^+e^- \rightarrow Z^0 + H^0)/\sigma_{\text{pt}}$ for different values of \sqrt{s} and m_H , taken from Ref. 22

We see that this reaction gives access to Higgs bosons with masses up to 100 GeV if LEP attains an energy of 100 GeV/beam. This reaction may therefore be the best window on m_H up to 100 GeV.

The measurement of the two Z^0 decay leptons determines the Z^0 mass:

$$m_Z \approx \sqrt{2E_{\ell^+}E_{\ell^-}(1 - \cos\theta_{\ell^+\ell^-})} \quad (2.39)$$

To estimate the energy of the lepton, Fig. 13 shows the variation of

$\epsilon_{\ell} \equiv E_{\ell}/m_Z + m_H$ as a function of $K \equiv \frac{\sqrt{s}}{m_Z + m_H}$ for three values of α , the lepton angle in the laboratory relative to the Z^0 direction. In the following table, the variation of the lepton energy is given for the four Higgs masses and \sqrt{s} values considered earlier.

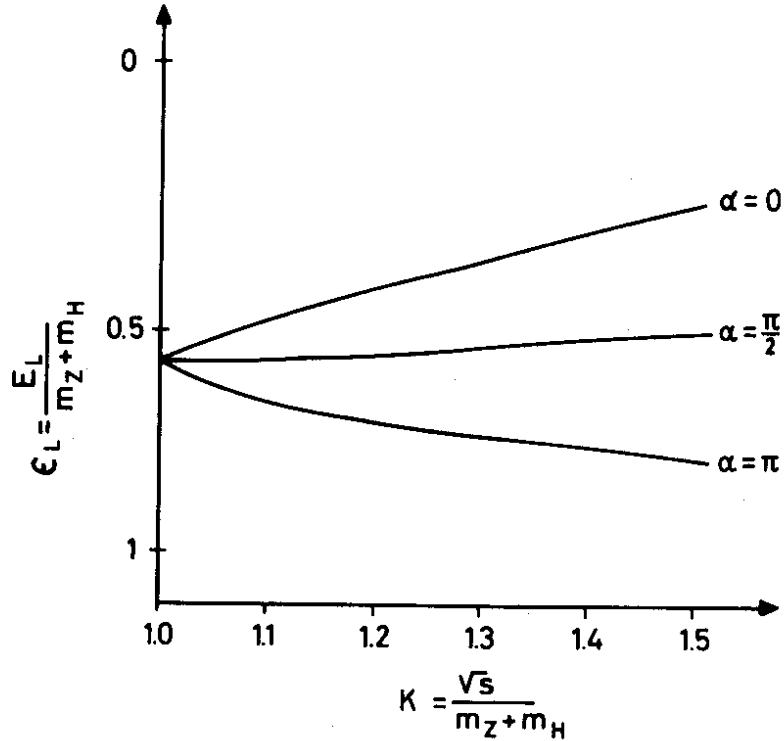


Fig. 13 - Values of ϵ_{ℓ} for different values of K and α . See the text.

Table - Kinematics for $e^+e^- \rightarrow Z^0 + H^0 \rightarrow e^+e^- + H^0$

m_H (GeV)	\sqrt{s} (GeV)	K	E_1^{\min} (GeV)	E_1^{\max} (GeV)	Δm_H (GeV)
10	104	1.04	40	50	25
30	132	1.10	45	65	8
45	154	1.14	50	75	5
60	175	1.17	52	87	4

As in the case of $Z^0 \rightarrow H^0 + \ell^+\ell^-$ considered earlier, the error on m_H is dominated by the error on the lepton energies:

$$\frac{\Delta m_Z}{m_Z} \approx \frac{1}{2} \left(\frac{\Delta E_{\ell^+}}{E_{\ell^+}} + \frac{\Delta E_{\ell^-}}{E_{\ell^-}} \right) \approx \frac{\Delta E_{\ell}}{E_{\ell}} \quad (2.40)$$

$$\text{and since } m_H^2 = m_Z^2 + s - 2E_Z \sqrt{s} \text{ we have } 2m_H \Delta m_H = 2m_Z \Delta m_Z + 2\sqrt{s} \Delta E_Z \quad (2.41)$$

If $\sqrt{s} \approx m_Z$, and observing that $\Delta E_Z \sim \Delta m_Z$ because of the natural width Γ_Z of the Z^0 , we find that

$$\Delta m_H \approx \frac{2m_Z}{m_H} \Delta m_Z \quad (2.42)$$

The table above lists the Δm_H obtained using the $Z^0 + e^+e^-$ signature which are also plotted in Fig. 14. The resolution obtained for $Z^0 + \mu^+\mu^-$ is considerably worse.

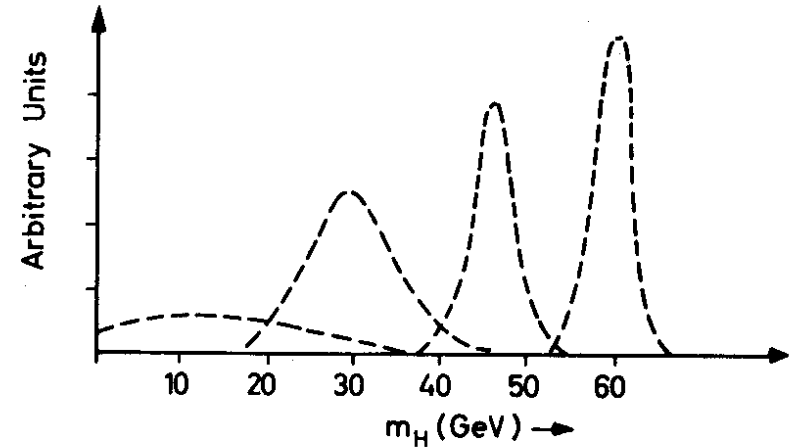


Fig. 14 - Resolution in m_H obtained using the e^{\pm} energy resolution (2.31)

As an example of a background to the reaction $e^+e^- \rightarrow Z^0 + H^0$ we consider the reaction

$$e^+e^- \rightarrow t\bar{t} X \rightarrow e^+e^- \nu\bar{\nu} b\bar{b} X \quad (2.43)$$

The effective cross section for this process can be written as:

$$\frac{\sigma(e^+e^- \rightarrow t\bar{t})}{\sigma_{pt}} \cdot [B(t \rightarrow eX)]^2 \approx 20R \cdot [B(t \rightarrow eX)]^2 \approx 0.2 R$$

at $\sqrt{s} = 104 \text{ GeV}$.

The cross section for producing two leptons according to 2.43 is therefore of the same order as the cross section for $e^+e^- \rightarrow Z^0 + H^0 \rightarrow (e^+e^-) + X$. However there are important kinematical differences between the two processes: the electrons from t decay will lead to a mixed hadron-lepton jet whereas the electrons from the Z^0 decay will in general be well separated from the hadron jets. Also electrons from t decay are soft compared to the electrons originating in the decay of a Z^0 nearly at rest. The effective mass spectra of these electrons will therefore peak well below the Z^0 mass as indicated in Fig. 15.

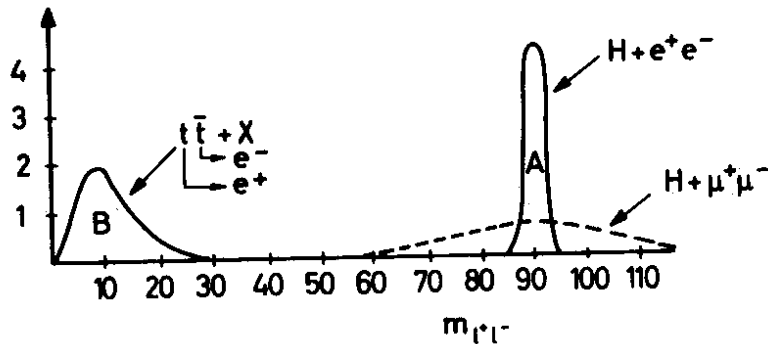


Fig. 15 - Lepton pair spectrum from $e^+e^- \rightarrow Z^0 + H^0$, $Z \rightarrow \ell^+\ell^-$, and from $e^+e^- \rightarrow t\bar{t} X$, $t \rightarrow e^+ X$, $\bar{t} \rightarrow e^- X$.

Note that the background resulting from radiative corrections to the Z^0 peak ($e^+e^- \rightarrow e^+e^- \gamma \rightarrow Z^0 \gamma$) can be excluded by a simple cut on multiplicity for $Z^0 \rightarrow e^+e^-$. The decay $Z^0 \rightarrow Q\bar{Q}$ can be removed by the cut on the lepton spectrum as discussed above in addition to a cut at the total energy observed in the final state.

We have seen that the reaction $e^+e^- \rightarrow Z^0 + H^0$ is relatively background-free. We also saw that the measurement of m_H through a missing mass technique can be achieved for $m_H > 20 \text{ GeV}$ by measuring electron energies, but not by measuring muon energies if we use $\Delta E_\mu/E_\mu \approx 0.15$ (2.32). For $m_H < 20 \text{ GeV}$ the missing mass method fails, so for light Higgs we would consider two alternative methods of search:

- (1) Look for a typical signature of a light Higgs such as $H^0 \rightarrow \tau^+\tau^-$ or $H^0 \rightarrow D\bar{D}X$. Experimentally, a clear signature would come from purely leptonic events such as

$$e^+e^- \rightarrow (\mu^+\mu^-) + e^\pm\mu^\mp \text{ (+ invisible neutrinos)}$$

The rate for 4 lepton events would be $O(1)/\text{day}$ for $m_H \approx 10 \text{ GeV}$.

- (2) The mass of the particle produced in the reaction

$$e^+e^- \rightarrow Z^0 + X \rightarrow (e^+e^-) + X$$

can be measured with a high accuracy ($\ll 1 \text{ GeV}$) by measuring the excitation curve close to threshold. We conclude that the reaction $e^+e^- \rightarrow Z^0 + H^0$ is a good way to look for H^0 in the mass range of 10 to 100 GeV.

2.6 Other Reactions

Several other processes have been proposed as means to find or study Higgs bosons. Most of these reactions seem less promising than the ones we have discussed previously, but some of them have interesting features.

$$e^+e^- \rightarrow H^0 + Q\bar{Q} \quad 23$$

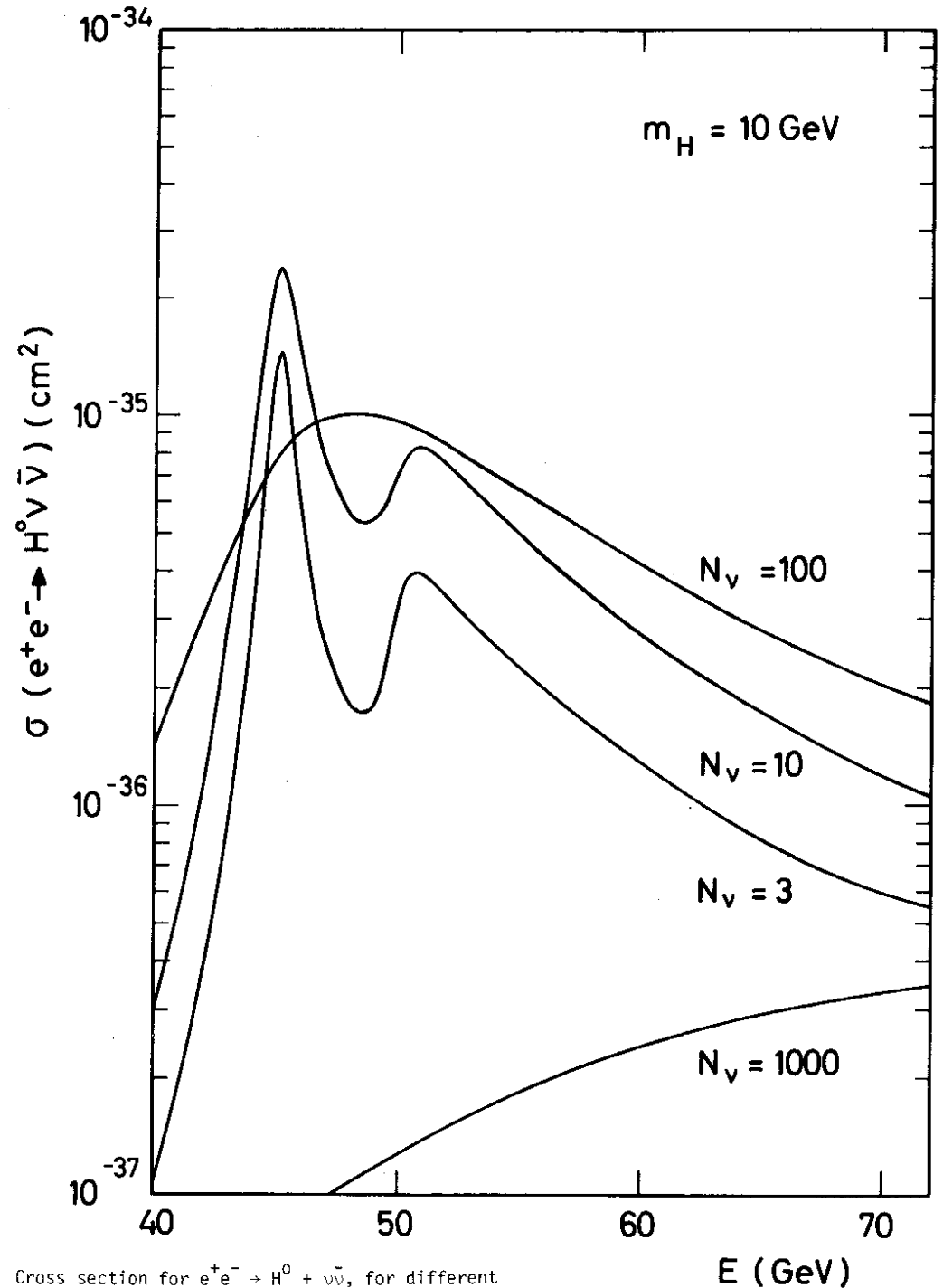
The idea is to use a heavy quark $Q\bar{Q}$ pair to bremsstrahl a Higgs boson, with an enhanced probability because of the larger coupling (2.13). Complete calculations exist only for $\sqrt{s} \ll m_Z$, where the cross section seems too small to be useful. The cross section is presumably largest on the Z^0 resonance peak, but seems unlikely to be competitive with the process $Z^0 \rightarrow H^0 + e^+e^-$ considered in section (2.4). The process might be interesting if there are very heavy fermions with masses $\geq m_Z$.

$$e^+e^- \rightarrow H^0 + \nu\bar{\nu} \quad 24$$

This reaction has been proposed as a method to count the number of neutrinos. If the existence and mass of a Higgs have been established in some other way, the production of heavy hadrons at large p_T with nothing else in the final state but large missing energy and momentum should be a sufficiently clean signature to identify the process. A representative set of cross section curves for different numbers of neutrinos N_ν are shown in Fig. 16

$$e^+e^- \rightarrow H^0 + H^0 + Z^0 \quad 25$$

This reaction has been proposed as a test of the $H^0H^0Z^0Z^0$ and $H^0H^0H^0$ couplings predicted by gauge theories. The cross section is not totally negligible, attaining almost $2 \times 10^{-38} \text{ cm}^2$ at a centre-of-mass energy of 130 GeV if $m_H = 10 \text{ GeV}$ (see Fig. 17). If the Higgs mass is sufficiently light, and some sort of distinctive decay signature can be found, it might be possible to detect this process, but it looks very marginal.



Cross section for $e^+e^- \rightarrow H^0 + \nu\bar{\nu}$, for different values of the beam energy E , and different values of N_ν , all with $m_H = 10 \text{ GeV}$. Taken from Ref. 24. **Fig.16**

$e^+e^- \rightarrow H^0 + \gamma$ off resonance ²⁶

The rate for this reaction close to an onium resonance has been found to be very small, and it does not seem to be a competitive way of looking for the H^0 .

$e^+e^- \rightarrow H^0 + f + \bar{f}$ off resonance ²⁷

In the previous sections we have considered $e^+e^- \rightarrow Z^0 \rightarrow H^0 + Z^0_{\text{virtual}} \rightarrow l^+l^-$ (section 2.4) and $e^+e^- \rightarrow Z^0_{\text{virtual}} \rightarrow H^0 + (Z^0 \rightarrow e^+e^-)$, i.e. processes where at least one on-shell Z^0 resonance is involved. The latter process gives access to H^0 with m_H up to $\sqrt{s}_{\text{max}} - 100$ GeV. Where \sqrt{s}_{max} is the maximum centre-of-mass energy accessible with LEP. In the present project this could be 240 GeV ²⁸, so that the range $m_H \leq 140$ GeV could be explored this way. One could in principle look at higher m_H by taking lepton pairs in the final state with invariant masses $< m_Z$. Important contributions to the cross-section might then be made by diagrams like that in Fig. 18, as well as by diagrams with two virtual Z^0 .

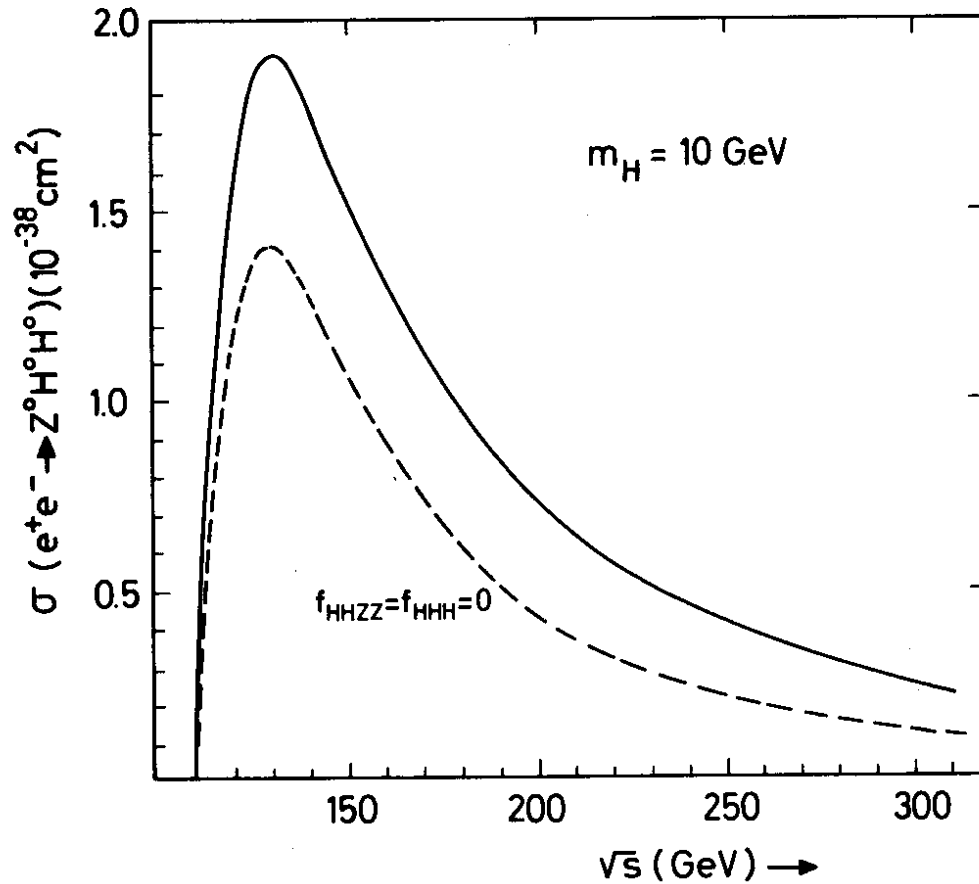


Fig. 17

Cross section for $e^+e^- \rightarrow H^0H^0Z^0$ as a function of the centre-of-mass energy $\sqrt{s} = 2E$, for $m_H = 10\text{GeV}$. Taken from Ref. 25. The dashed line corresponds to setting the $H^0H^0Z^0Z^0$ and $H^0H^0H^0$ couplings to zero

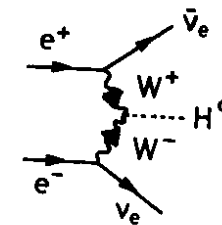


Fig. 18 - Diagram for H^0 production in association with a $\nu_e\bar{\nu}_e$ pair.

If one accepts the observability of a cross section as low as 10^{-38} cm², then, as shown ²⁷ in Fig. 19 \sqrt{s}_{max} would allow access to m_H up to about 160 GeV. The dominant reaction then has $H^0 + (\nu\bar{\nu})$ final states, which could be identified by the large missing energy/momentum of the neutrinos.

Indirect effects of Heavy H^0

If m_H is heavier than ~ 160 GeV, we see no way of producing it directly at LEP, and are reduced to looking for indirect manifestations of its effects in higher orders of perturbation theory. It has been suggested²⁹ that the process $e^+e^- \rightarrow W^+W^-$ might be sensitive to $m_H > 300$ GeV, but no detailed calculations of Higgs effects on this process have yet been completed. More theoretical work on this process is necessary before we can conclude whether LEP can explore the full range $7.3 \text{ GeV} < m_H < 1 \text{ TeV}$ allowed by present theoretical constraints.

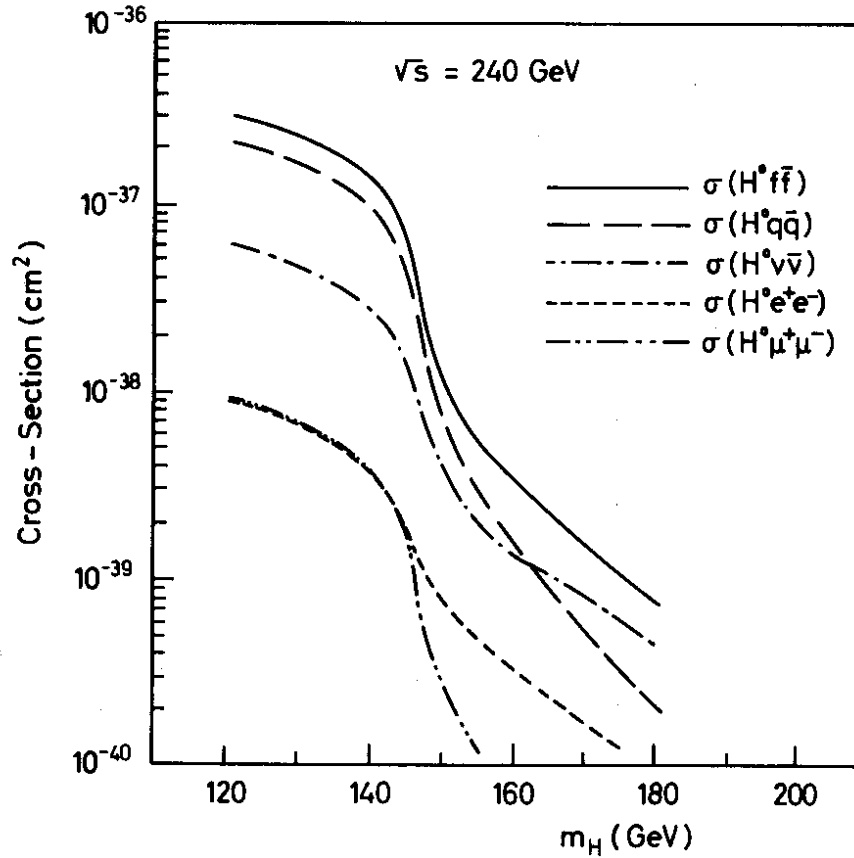


Fig. 19

Total cross-section for $e^+e^- \rightarrow H^0 f\bar{f}$ at $\sqrt{s} = 240$ GeV, for large Higgs masses. Taken from Ref. 27.

3. Charged Higgs Particles

3.1 Motivations and Properties

Charged Higgs particles are not present in the minimal Weinberg-Salam theory which just has one Higgs doublet, as discussed in section 2. However, this is definitely the exception: Gauge theories based on groups bigger than $SU(2) \times U(1)$ contain charged Higgs particles, and so do non-minimal Weinberg-Salam models with more than one Higgs multiplet. The couplings of these Higgs particles are not so precisely fixed² as in the minimal model. However, the belief that all fermions acquire their masses from their couplings to Higgs fields suggests that, other things being equal, $Hf\bar{f}$ couplings will be qualitatively analogous to (2.8). Thus couplings to heavier fermions are expected to be larger, though this could easily be modified by mixing factors analogous, and perhaps similar in origin, to the generalized Cabibbo weak mixing angles. As a working hypothesis, we therefore expect that light charged Higgs particles ($m_H \pm < 10$ to 20 GeV) will have preferred decay modes

$$H^+ \rightarrow t^+ \bar{b}, \quad H^+ \rightarrow c \bar{s} \quad (3.1)$$

presumably with similar rates. The decay $H^+ \rightarrow c \bar{s}$ may lead to final states of the form

$$H^+ \rightarrow D^+ K^0 \text{ or } H^+ \rightarrow F^+ \text{ (} \eta \text{ or } \eta' \text{ or } \phi \text{)} \quad (3.2)$$

which could allow the mass of the charged Higgs to be reconstructed from the hadrons in the final state.

However the branching ratios for these exclusive modes will decline as m_H increases. For heavier H^+ the preferred decay modes may well be $H^+ \rightarrow t \bar{b}$. As in the case of neutral Higgs particles, we feel that this preference for decay into the heaviest particles available may well provide useful signatures. We recall that the mass of a neutral Higgs was very difficult to estimate theoretically. The same is even more true of charged Higgs particles. We have a vague prejudice that their masses may be of order 10 to 10^2 GeV, but no good rationale for this belief.

We now turn to the discussion of H^\pm production mechanisms.

3.2 $e^+e^- \rightarrow H^+H^-$

Charged Higgs particles are pointlike scalar particles and can be pair-produced by the diagrams in Fig. 20. The cross-section for this process can be written as

$$\frac{\sigma(e^+e^- \rightarrow H^+H^-)}{\sigma_0} = 1 - \frac{2s \chi v v_H}{(s/m_Z^2 - 1) + \Gamma_Z^2/(s - m_Z^2)} + \frac{s^2 \chi^2 (v^2 + a^2) v_H^2}{(s/m_Z^2 - 1) + \Gamma_Z^2/m_Z^2} \quad (3.3)$$

where σ_0 is the QED cross section;

$$\sigma_0 (e^+e^- \rightarrow \gamma \rightarrow H^+H^-) = \frac{\pi \alpha^2 \beta^3}{3s} = 21.9 \left(\frac{\beta^3}{s} \right) \text{ nb} \quad (3.4)$$

with

$$\chi \equiv \frac{G_F}{8\sqrt{2} \pi \alpha} = 4.47 \times 10^{-5} \text{ GeV}^{-2} \quad (3.5)$$

and $\beta = P_H/E_H$

We take $\sin^2\theta = 0.20$, which conflicts neither with theoretical ideas nor recent data, corresponding to

$$m_Z = 93.5 \text{ GeV}, \quad a = -1, \quad v = -0.2 \quad \text{and} \quad v_H = -0.2 \quad (3.6)$$

Assuming three generations of fundamental fermions we find

$$\Gamma_Z \approx 3.0 \text{ GeV}.$$

The cross-section given by (3.3) is plotted in Fig. 21 as the solid line. The dotted line gives the cross-section expected from the photon annihilation diagram alone. We note that the photon exchange diagram dominates everywhere except close the Z^0 pole. The rates for $m_H = 10$ GeV and 50 GeV calculated using the luminosity quoted for LEP 70 are listed in the Table below.

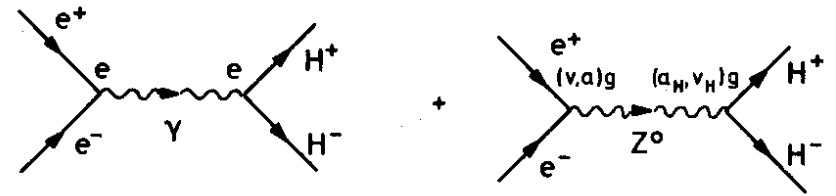


Fig. 20 - Diagrams contributing to $e^+e^- \rightarrow H^+H^-$

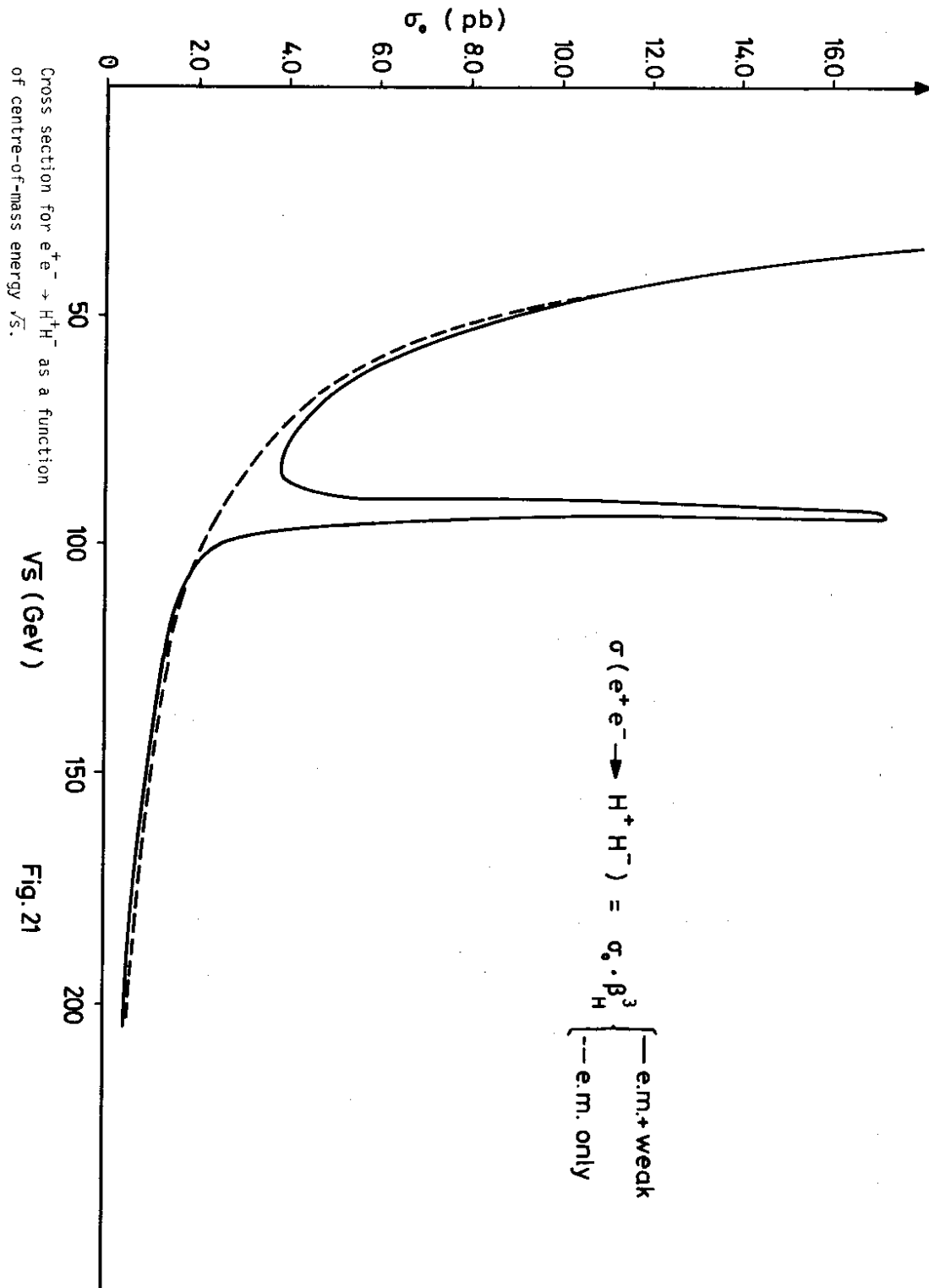


Table - Events/day for $e^+e^- \rightarrow H^+H^-$ with LEP 70

\sqrt{s} (GeV)	70	85	90	93.9	97	100	110	120	140	160	180	200
$m_H=10\text{GeV}$	8.8	11.3	19.4	61.8	15.1	10.3	8.9	8.9	9.0	6.0	3.3	1.9
$m_H=50\text{GeV}$							0.7	1.6	3.2	2.9	2.0	1.2

These rates are not very large and represent only a few percent of the total hadronic cross-section. Near threshold, however, they will give rise to events with high sphericity and may thus be separated from the bulk of the hadronic events. The H^+H^- events will have a distinctive angular distribution $\sim (1 - \cos^2\theta)$.

The slow rise of the cross-section with energy ($\sim \beta^3$), the absence of any 1^{--} resonant states, and the absolute magnitude as well as the angular distribution might be used to separate $e^+e^- \rightarrow H^+H^-$ from the production of heavy $Q\bar{Q}$ pairs. The decay $H^\pm \rightarrow (\text{hadrons})$ may be used to determine the mass independently from the threshold determination.

The low rate makes it seem unlikely that pair-production can be used to find charged Higgs bosons with masses much above 50 GeV. Also we will see in a moment more promising approaches to the search for H with masses up to $O(100)$ GeV.

3.2 $e^+e^- \rightarrow W^\pm H^\mp$ ⁹

Gauge theories predict that if there is a charged Higgs then it should have a coupling $H^- Z^0 W^+$ of the general form

$$K_{ZWH} g_W^H \left[Z_\mu^0 W^{+\mu} H^- + (\text{hermitian conjugate}) \right] \quad (3.7)$$

where one's general prejudice is that $K_{ZWH} = O(1)$. The process $e^+e^- \rightarrow Z^0 \rightarrow W^+H^-$ can therefore proceed as shown in Fig. 22, which gives a cross section

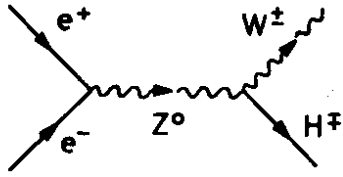


Fig. 22 - Diagram contributing to $e^+e^- \rightarrow W^+H^-$

$$\sigma(e^+e^- \rightarrow W^+H^-) = \frac{K_{ZWH}^2 \alpha^2 \pi^2 (a^2 + v^2)}{m_W^2 \sin^4 \theta_W} \left[\frac{m_W^2}{m_Z^2 - s} \right]^2 \times \left[1 - \frac{2(m_W^2 + m_H^2)}{s} + \frac{(m_W^2 - m_H^2)^2}{s^2} \right]^{1/2} \quad (3.8)$$

The cross section (3.8) is plotted in Fig. 23 for $m_H = 10$ GeV, 50 GeV and $m_H = m_W = 83.6$ GeV. Note the characteristic shape and large magnitude of the cross-section near threshold for a low Higgs mass. The rates for $e^+e^- \rightarrow W^+H^-$, assuming $K_{ZWH} = 1$ and the luminosity given for LEP 70, are listed in the Table below:

Table - Events/day for $e^+e^- \rightarrow W^+H^-$

\sqrt{s} (GeV)	100	110	120	140	160	180	200
$m_H = 10$ GeV	15700	4378	2331	1093	448	172	73
$m_H = 50$ GeV				504	331	146	65
$m_H = 83.6$ GeV						81	47

Cross section for $e^+e^- \rightarrow W^+H^-$ as a function of centre-of-mass energy \sqrt{s} .

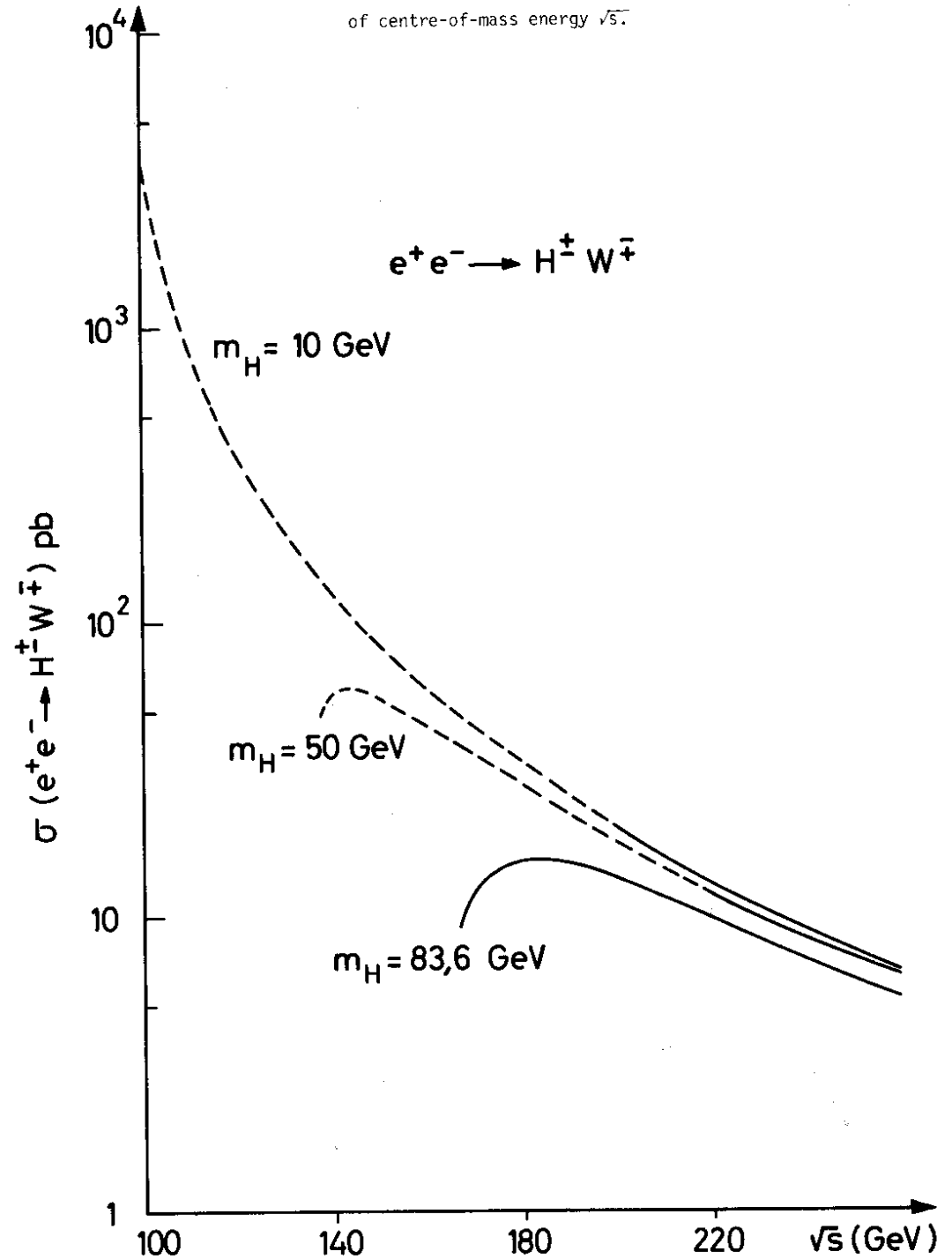


Fig. 23

The best signature for this process is depicted in Fig. 24. We expect that about 16% of the reactions will yield a high energy μ or e , recoiling against a τ or hadronic final state, and with a large missing energy carried off by a ν . Close to threshold the e or μ will be almost monochromatic with $E \sim m_{W/2} \sim 42$ GeV.

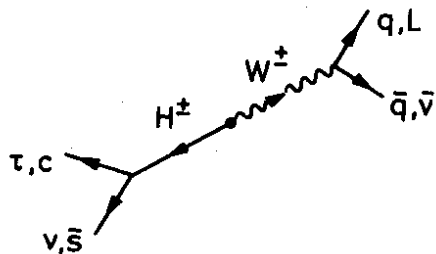


Fig. 24 - Signature for $e^+e^- \rightarrow W^+ H^-$

This seems a distinctive signature. The rates are sufficient to explore the charged Higgs sector up to 90 GeV with LEP 70, and well beyond 100 GeV with LEP -8.

We conclude that $e^+e^- \rightarrow W^+ H^-$ is a better reaction than $e^+e^- \rightarrow H^+H^-$ for searching for charged Higgs particles.

3.3 Heavy quark decays to $H^+ + q$ ⁸

The predominant mechanism for weak heavy quark decay is generally expected to be that depicted in Fig. 25a, for which the total width is approximately given by

$$\Gamma(Q \rightarrow qq\bar{q} + q\ell\bar{\nu}) \approx \frac{G_F^2 m_Q^5}{192\pi^3} (3N_{qD} + N_{\ell D}) \quad (3.9)$$

where N_{qD} is the number of weak quark doublets, and $N_{\ell D}$ is the number of weak lepton doublets. If charged Higgs particles do exist then the semiweak decay mode shown in Fig. 25 b is also possible. The corresponding decay

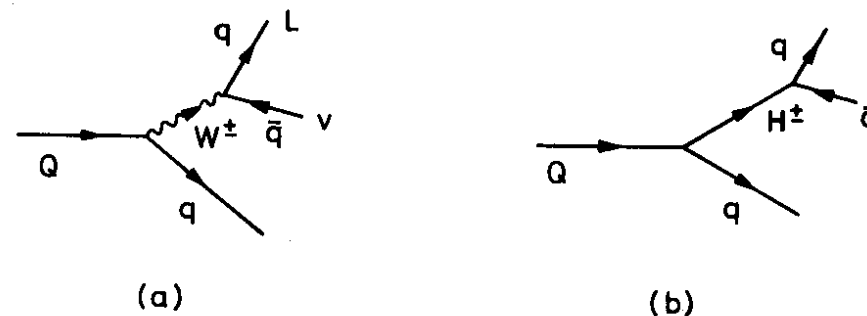


Fig. 25 - Dominant contributions to heavy quark decay: (a) through intermediate (virtual) W^+ , (b) into $H^+ + q$

rate is given by

$$\Gamma(Q \rightarrow H^+q) = \frac{G_F^2 m_Q^3}{32\pi} \cdot K_{Hf\bar{f}}^2 \quad (3.10)$$

where one is prejudiced to believe that $K_{Hf\bar{f}}^2 = O(1)$ in the absence of unfriendly mixing angles. The ratio between the decay modes (3.9) and (3.10) is

$$\frac{\Gamma(Q \rightarrow H^+q)}{\Gamma(Q \rightarrow qq\bar{q} + q\ell\bar{\nu})} = \frac{6\pi^2}{G_F^2 m_Q^2 (3N_{qD} + N_{\ell D})} \quad (3.11)$$

Assuming 3 generations of fermions in (3.11) we find

$$\frac{\Gamma(Q \rightarrow H^+q)}{\Gamma(Q \rightarrow qq\bar{q} + q\ell\bar{\nu})} = \frac{4.8 \times 10^{-5}}{m_Q^2} \quad (3.12)$$

The total decay width and the ratio of these decay modes are listed below as a function of quark mass.

Table - Weak decays of heavy quarks

m_Q (GeV)	$\Gamma(Q \rightarrow H^\pm q)$ (MeV)	$\Gamma(Q \rightarrow qq\bar{q} + q\ell\bar{\nu})$ (MeV)	$\Gamma(H^\pm q) \Gamma(qq\bar{q} + q\ell\bar{\nu})$
15	0.4	2×10^{-4}	2×10^3
30	3	6×10^{-3}	5×10^2
60	24	0.2	120
80	98	1	60

When $m_Q > m_W$ the decay $Q \rightarrow W^\pm + q$ becomes kinematically accessible and will be competitive with $Q \rightarrow H^\pm + q$.

If we assume that the $Q H^\pm q$ coupling is not strongly reduced by the equivalent of Cabibbo angles, the decay $Q \rightarrow H^\pm q$ is clearly dominant for $m_Q < m_W$. Indeed, the decay $c \rightarrow H^+ + (\bar{s} \text{ or } \bar{d})$ would completely dominate the decay of charmed mesons, and give them lifetimes $\ll 10^{-13}$ seconds if m_{H^+} were < 1 GeV. The observation of charmed particles with lifetimes $O(10^{-13} \text{ to } 10^{-12})$ seconds can therefore be used to exclude the existence of a charged Higgs particle with $m_{H^+} < 1$ GeV, assuming that the angle factor is not $\ll 1$.

The decay $Q \rightarrow H^\pm q$ will show up in:

a) $e^+e^- \rightarrow Q^+Q^- \rightarrow H^+H^- + q\bar{q}$

These processes will give rise to rather isotropic events, quite often with mixed hadrons and leptons. However, such final states are also expected from the normal $Q \rightarrow qq\bar{q}$ decays of heavy quarks, so that these will not be easily identifiable sources of H^\pm particles.

b) $e^+e^- \rightarrow \text{Onium} \rightarrow H^+H^- + q\bar{q}$ ³⁰

The decay rates in the table above indicate that the decay of heavy quarks $Q \rightarrow H^\pm +$ light quarks may proceed faster than the decay of $Q\bar{Q}$ bound states, which are expected to be $O(10 \text{ KeV to } 1 \text{ MeV})$. If a heavy Q or \bar{Q} in an onium bound state decays before the onium decays into gluons as conventionally expected,

the signatures will be distinctive. First, the width of the resonance will be much larger than that expected from $1^{--} \rightarrow 3 \text{ gluons} \rightarrow \text{hadrons}$. Secondly, it will lead to an unexpectedly large fraction of final states with mixed leptons and hadrons on resonance. Thirdly, it will give hadronic final states with large acoplanarity (from $V \rightarrow Q\bar{Q} \rightarrow H^-q \rightarrow H^+H^- + qq \rightarrow qq\bar{q} + \bar{q}q\bar{q}$) whereas conventional $V \rightarrow 3 \text{ gluon}$ decays are expected to yield a predominance of planar events. Present measurements of T decays in e^+e^- annihilation are not yet sufficiently precise to exclude a contribution from $H^+H^- + X$ decays at the rate expected, particularly in view of the possibility of suppression by Cabibbo-like angles. Listed in the table below are the rates of production of 1^{--} onia in e^+e^- collisions, assuming the luminosity given for LEP 70:

Table - Onium event rates/day

m_V (GeV)	40	60	80	100	120	140	180
	260	170	140	105	90	7.5	1.7

Although the $Q \rightarrow H^\pm + q$ decays, if present, will greatly increase the width of the onium resonance, it will still be considerably less than the expected resolution of the beam energies, so that the event rates are not affected thereby.

We conclude that onium decays are a good way to look for light charged particles with masses $< \frac{1}{2} m_V$, m_V being the onium mass.

4. Conclusions

Our major conclusion is that experiments at LEP should be able to detect the existence of any Higgs boson - either neutral or charged - with a mass up to ~ 100 GeV. The ranges accessible via different production reactions are shown in Figs. 26 and 27.

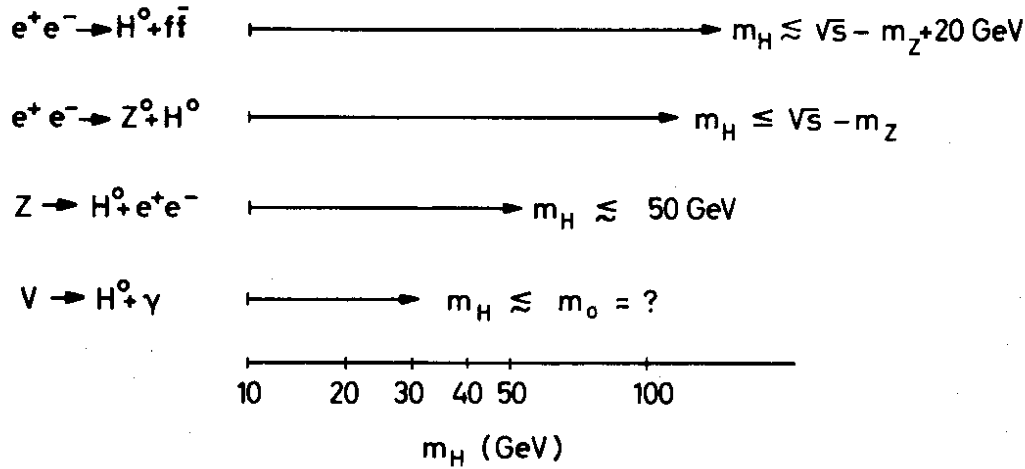


Fig. 26 - Useful production mechanisms for neutral Higgs particles

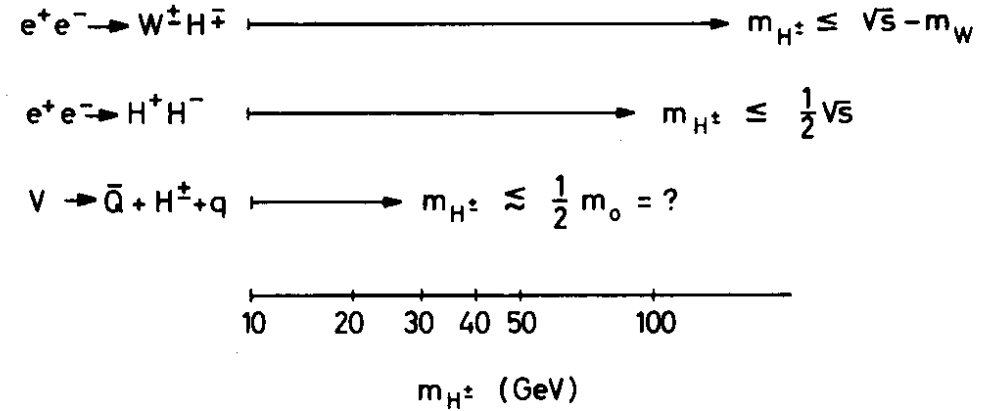


Fig. 27 - Useful production mechanisms for charged Higgs particles

Neutral Higgs:

The best production process seems to be $e^+e^- \rightarrow Z^0 + H^0$, which should give reasonable event rates for m_H up to $\sqrt{s}_{\max} - M_Z$. Even if a clear signature from H^0 decay is not available, the decays $Z^0 \rightarrow e^+e^-$ or $\mu^+\mu^-$ should provide a clear signature for this reaction. The mass of the Higgs could be measured quite precisely from the threshold behaviour. Higgs with masses up to 50 GeV could also be produced at reasonable rates in Z^0 decays via the reaction $Z^0 \rightarrow H^0 + (e^+e^-)$ or $(\mu^+\mu^-)$. Here the background problems (e.g. from $Z^0 \rightarrow t\bar{t}$, $t \rightarrow \ell^+\chi$, $t^- \rightarrow \ell^-\chi$) are more severe than for the $e^+e^- \rightarrow Z^0 + H^0$ reaction. Nevertheless, it seems possible to dig out an H^0 signal, and this might be the best way to look for high mass Higgses if LEP is restricted to ≤ 75 GeV per beam in an initial phase. By comparison, the decay $Z^0 \rightarrow H^0 + \gamma$ seems to suffer from lower event rates than $Z^0 \rightarrow H^0 + \ell^+\ell^-$, and a worse electromagnetic background problem. It is not clear to us how the $Z^0 \rightarrow H^0 + \gamma$ process could be detected. Another competitive reaction for H production would be onium $V \rightarrow H^0 + \gamma$ if there exists an onium in the LEP centre-of-mass energy range.

This reaction would have low background and an acceptably high event rate, but we cannot of course know whether it will be kinematically available.

If no neutral Higgs is found with $m_H < \sqrt{s}_{\max} - m_Z$, it may be possible to increase the accessible range of m_H by looking for $e^+e^- \rightarrow H^0 + (\text{non-resonant}) f\bar{f}$, which might be usable for m_H up to $\sqrt{s}_{\max} - m_Z + 20$ GeV. However, such a search would be rather a desperate business!

The accessibility of H^0 production at LEP by various different mechanisms (see Fig. 26) and the possibility of observing its different decay modes suggest that experiments at LEP should not only be able to verify the existence of a neutral Higgs particle, but also determine at least the gross feature of its coupling to other particles, and verify whether they are consistent with the expected forms (2.13, 2.14).

Charged Higgs:

The best production process may be $e^+e^- \rightarrow W^\pm + H^\mp$, which has a reasonable event rate for any H^\pm with mass $< \sqrt{s}_{\max} - m_W$. Furthermore this process has a distinctive signature from the leptonic decays of the W^\pm . As for the $e^+e^- \rightarrow Z^0 + H^0$ reaction, the threshold behaviour should give us an accurate measure of m_{H^\pm} . The cross-sections are very large close to threshold for a light H^\pm , because of the nearby Z^0 pole just below threshold. The reaction $e^+e^- \rightarrow H^+H^-$ is also in principle a good way to look for $m_{H^\pm} < 50$ GeV. The reaction can be distinguished from a heavy $Q\bar{Q}$ threshold by three features: its threshold behaviour $\sim \beta^3$, its angular distribution $\sim (1 - \cos^2\theta)$, and the absence of onium bound states just below threshold. Clearly, however, detecting $e^+e^- \rightarrow H^+H^-$ will be hard if there are very many other thresholds for heavy leptons or quarks in the LEP energy range.

On the other hand, if a very heavy quark or lepton exists, its decays into charged Higgs particles are probably substantial. The decay rate $Q \rightarrow H^\pm + q$ is much more rapid than $Q \rightarrow (\text{virtual } W^\pm) + q$, $(\text{virtual } W^\pm) \rightarrow q + \bar{q}$. Picking out $H^\pm + q$ decays of heavy quarks Q above threshold may be difficult, but the process $Q \rightarrow H^\pm + q$ goes so fast that it even becomes a competitive or dominant decay mode of the onium itself: $V \rightarrow \bar{Q} + H^\pm + q$. This would give onium final states with high acoplanarity feature not expected from conventional $V \rightarrow 3$ gluon decay.

We therefore feel that if a charged Higgs particle exists with mass up to ~ 100 GeV, experiments at LEP should be able to find it, via the reactions shown in Fig. 27.

REFERENCES

- 1 - S. Weinberg - Phys.Rev.Lett. 19, 1264 (1967);
A. Salam - Proceedings of the 8th Nobel Symposium on Elementary Particle Theory, Relativistic Groups and Analyticity, ed. by N. Svartholm (Almqvist and Wiksells, Stockholm, 1968), p. 367.
For a phenomenological review and references, see
J. Ellis - Proceedings of the 1978 SLAC Summer Institute, SLAC - 215 (1978), also available as SLAC-PUB-2177.(1978).
- 2 - For a review and references, see
M.K. Gaillard - Comments on Nuclear and Particle Physics 8, 31 (1978).
- 3 - For earlier discussions of Higgs particles at LEP, see
L. Camilleri et al. - CERN Yellow report 76-18 (1976), especially section III;
Proceedings of the LEP Summer Study - CERN Yellow report 79-01 (1979), especially section 1-14.
- 4 - F. Wilczek - Phys.Rev.Lett. 39, 1304 (1977).
- 5 - R.N. Cahn, M.S. Chanowitz and N. Fleishon - LBL-8495 (1978)
- 6 - J.D. Bjorken - Proceedings of the 1976 SLAC Summer Institute, SLAC-198 (1978) also available as SLAC-PUB-1866 (1977).
- 7 - J. Ellis, M.K. Gaillard and D.V. Nanopoulos - Nucl. Phys. BI06, 292 (1976)
- 8 - E. Golowich and T.C. Yang - Univ. of Massachusetts preprint "Charged Higgs bosons and decays of heavy flavoured mesons" (1978).
- 9 - J.F. Donoghue and L.-F.Li - Carnegie-Mellon University preprint COO- 3066-113 (1978).

PR D18 945 (78)

- 10 - G. 't Hooft - Nucl.Phys. B39 , 167 (1971).
- 11 - C.H. Llewellyn Smith - Phys.Lett. 46B, 233 (1973);
J.S. Bell - Nucl.Phys. B60, 427 (1973);
J.M. Cornwall, D.N. Levin and G. Tiktopoulos -
Phys.Rev.Lett. 30 , 1268 (1973).
- 12 - See for example L.Susskind - SLAC-PUB 2142 (1978) and
S.Dimopoulos and L.Susskind
- 13 - B.W. Lee, C. Quigg and H.B. Thacker - Phys.Rev.Lett. 38, 883 (1977);
C.E. Vayonakis - Lett. al. Nuovo Cimento 17, 383 (1976) and
Athens University preprint "New Threshold of Weak Interactions" (1978);
M. Veltman - Acta Physica Polonica B8, 475 (1977).
- 14 - S. Coleman and E. Weinberg -Phys.Rev. D7, 1888 (1973).
- 15 - E. Gildener and S. Weinberg -Phys.Rev. D13, 3333 (1976).
- 16 - J. Ellis, M.K. Gaillard, D.V. Nanopoulos and C.T. Sachrajda
-CERN TH-2634 (1979).
- 17 - S. Weinberg - Phys.Rev.Lett. 36, 294 (1976);
A.D. Linde - JETP Lett. 23, 64 (1976).
- 18 - P.H. Frampton - Phys.Rev.Lett. 37, 1378 (1976).
- 19 - A.D. Linde - Phys.Lett. 70B, 306 (1977).
- 20 - B.H. Wiik - Proceedings of the LEP Summer Study, ref. 3.
- 21 - J. Finjord - CERN preprint TH.2663 (1979)
- 22 - For more detailed discussions of the cross-section for this
process, see
B.W. Lee, C. Quigg and H.B. Thacker -Phys.Rev. D16 1519 (1977);
S.L. Glashow, D.V. Nanopoulos and A. Yildiz - Harvard University
preprint HUTP-78/A012 (1978).
- 23 - K.J.F. Gaemers and G.J. Gounaris -
- 24 - A. Van Proeyen - Leuven preprint KUL-TF-78/030 (1978).
- 25 - G.J. Gounaris, D. Schildknecht and F.M. Renard-Bielefeld preprint
ECFA/LEP Working Group SSG/9/2, BI-TP 79/02 (1979).
- 26 - J.P. Leveille - Wisconsin preprint C00-881-86 (1979)
- 27 - D.R.T. Jones and S.T. Petcov - CERN TH Internal report,
ECFA/LEP Working Group SSG/9/3 (1979).
- 28 - W. Schnell - CERN-ISR-RF/79-3 (Contribution to the 1979
Particle Accelerator Conference - San Francisco, March (1979).
See also:
The LEP Study Group - Design Study of a 15 to 100 GeV e^+e^-
Colliding Beam Machine (LEP) - CERN Internal Report ISR LEP/78-17
(1978).
- 29 - M. Veltman - many private communications.
- 30 - J.Ellis, ref. 1.